

Instituto Tecnológico de Costa Rica
Escuela de Ingeniería Electrónica
Programa de Maestría en Ingeniería Electrónica con Énfasis en Sistemas
Microelectromecánicos

“Estudio Mediante Simulaciones de las Propiedades Eléctricas
de la Interfaz Gel-Piel Durante la Estimulación Eléctrica
Neuromuscular”

para optar por el título de

Magister en Ciencias en Ingeniería Electrónica

con el grado académico de

Maestría

David Leonardo Sánchez Ordoñez

Cartago Abril, 2014

Instituto Tecnológico de Costa Rica
Electronics Engineering Department
Master's Program in Electronics Engineering



Simulation Study of the Electrical Properties of Gel-Skin Interface during Neuromuscular Electric Stimulation

Master's Thesis in fulfillment of the requirements for the degree of

Master on Science in Electronics Engineering
Microelectromechanical Systems Major

Submitted by
David Leonardo Sánchez Ordoñez

April, 2014

I declare that the present Master's Thesis has been realized entirely by me, using and applying literature relevant to the theme and introducing my own knowledge.

In the cases where bibliography was used, I have properly provided the sources through the respective bibliographic references. In consequence, I assume total responsibility for the Master's Thesis realized and for the content of the corresponding final report.

David Leonardo Sánchez Ordoñez

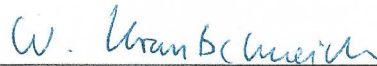
San José, April 22nd 2014

ID Number: 186200355800

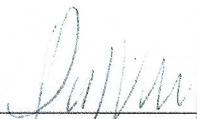
Instituto Tecnológico de Costa Rica
Electronics Engineering Department
Master's Thesis
Examination Committee

This Master's Thesis is presented before the following Examination Committee as a requisite to opt for the degree of Master on Science in Electronics Engineering of Instituto Tecnológico de Costa Rica.

Members of the Committee



Prof. Dr.-Ing. Wolfgang Krautschneider
Reviewer


Dr.-Ing. Paola Vega Castillo
Reviewer

Dr. Bruno Chine Polito
Reviewer



MSc. Diego Luján Villarreal
Advisor

The members of this Committee testify that the presented Master's Thesis has been approved and complies with the established regulations dictated by the School of Electronics Engineering.

San José, April 22nd 2014

INSTITUTO TECNOLÓGICO DE COSTA RICA
ESCUELA DE INGENIERÍA ELECTRÓNICA
TESIS DE MAESTRÍA EN ELECTRÓNICA
TRIBUNAL EVALUADOR
ACTA DE EVALUACIÓN

Tesis de Maestría defendida ante el presente Tribunal Evaluador como requisito para optar por el título de Máster en Ingeniería Electrónica con énfasis en Sistemas Microelectromecánicos del Tecnológico de Costa Rica.

Estudiante: David Sánchez Ordoñez

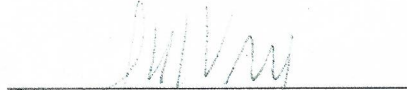
Nombre de la Tesis: **Stimulation study of the electrical properties of the gel-skin interface during neuromuscular electric stimulation**

Miembros del Tribunal



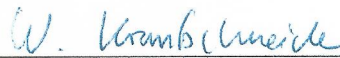
Dr. Bruno Chiné

Profesor lector



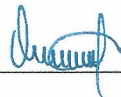
Dr-Ing. Paola Vega Castillo

Profesor Lector



Dr-Ing. Wolfgang Krautschneider

Profesor lector



M.Sc. Diego Luján Villarreal

Profesor asesor

Los miembros de este Tribunal dan fe de que el presente trabajo de graduación ha sido aprobado y cumple con las normas establecidas por la Escuela de Ingeniería Electrónica

Nota Final de la Tesis de Maestría : 90

Cartago, 2 de Mayo, 2014

Resumen

La presente Tesis de Maestría aborda el área de Estimulación Eléctrica NeuroMuscular (NMES por sus siglas en inglés), la cual consta de la activación de fibras nerviosas y musculares por medio de la aplicación de pulsos eléctricos usando dos electrodos colocados sobre la piel. La NMES es utilizada como entrenamiento muscular, rehabilitación y una herramienta de recuperación después del ejercicio. Un gel conductor es utilizado entre el electrodo y la piel para obtener una impedancia de contacto menor y evitar daños cutáneos, sin embargo, estos sistemas todavía deben mejorar en la obtención de una distribución uniforme de la corriente a lo largo de los electrodos. Por tanto, surge la necesidad de estudiar las características eléctricas de la interfaz entre el electrodo y la piel. En la presente Tesis de Maestría se describe y desarrolla un modelo 3D de elementos finitos basado en parámetros obtenidos experimentalmente y de referencias bibliográficas para simular el comportamiento eléctrico de esta interfaz y así obtener dichas características. Una serie de simulaciones son realizadas para determinar el conjunto de parámetros de señal y configuración de electrodos que logran una distribución más equitativa a lo largo de la interfaz gel-piel concluyendo con lineamientos a tener en cuenta para obtener dicha distribución.

Palabras Clave: NMES, Modelo de Elementos Finitos, Interfaz Gel-Piel

Abstract

The following Master's Thesis engages in the area of NeuroMuscular Electrical Stimulation (NMES), which comprises the activation of nerves and muscle fibers by applying electrical current pulses using two electrodes placed on the skin. NMES has great potential to serve as strength training, rehabilitation and post-exercise recovery tool. A conductive electrolyte (gel) is applied between the electrodes and the skin to obtain lower contact impedance and prevent skin damage; nevertheless, these systems need to improve to obtain a more uniform distribution of the electric current throughout the electrodes. Therefore, the need to study the electrical characteristics of the gel-skin interface arises. In this Master's Thesis a 3D Finite Element Model based on experimentally obtained parameters is described and developed to simulate the electrical behavior of the gel-skin interface and obtain said characteristics. A series of simulations are performed to determine the group of signal parameters and electrode configuration that achieve the best uniformity in electrical current distribution throughout the gel-skin interface. In the end, the guidelines to obtain said uniform distribution are listed.

Keywords: NMES, Finite Element Model, Gel-Skin Interface

To God, for always keeping me healthy, allowing me to work hard

*To the best parents in the world, my parents, always guiding me through life and
teaching me how to do everything with passion*

*To my beloved bother, you always make me want to be a better example for you,
let's keep growing little bother!*

Acknowledgement

This Thesis wouldn't have been possible without the support and advice from so many people that were my guardians:

My family, always looking for ways to help me and give me advice

My girlfriend, Laura, with her love and patience she always kept me motivated

Dr.-Ing Paola Vega, my mentor through the whole way, an incredible researcher and teacher and always the bearer of the best advices,

Prof. Dr-Ing Wolfgang Krautschneider, allowing me to ally with the Institute of Nanoelectronics of the Technische Universität Hamburg-Harburg, making possible the development of this Master's Thesis,

Thank you all!

Table of Contents

Figure Index	iii
Table Index	v
1 Introduction	1
1.1 Objectives.....	2
1.2 Structure of the Thesis	3
2 Theoretical Background	4
2.1 Neuromuscular System	4
2.1.1 Nerve Fiber Electrophysiology	4
2.1.2 Skeletal Muscle Contraction.....	6
2.2 Electrical Stimulation	7
2.2.1 Methods and Applications of Electrical Stimulation.....	7
2.2.2 Recruitment Patterns Under NMES.....	9
2.2.3 Signal Conditions and Strength-Duration Curve.....	10
2.3 Electrical Properties of Materials Involved.....	11
2.3.1 Electrode and Electrolyte	12
2.3.2 Skin.....	13
2.3.3 Muscles and Bones	15

2.4	Modeling Human Tissues	16
2.4.1	COMSOL Electric Currents Interface.....	19
3	Finite Element Model.....	22
3.1	Parameters	22
3.2	Stimulation Signal.....	23
3.3	Geometry	25
3.4	Materials	27
3.5	Meshing	28
3.6	Boundary Conditions	30
3.7	Study and Solver Configurations	31
4	Results and Analysis	33
4.1	Electrical Potential Distribution.....	33
4.2	Current Density Distribution.....	40
4.3	Total Power Dissipation	46
5	Conclusions and Recommendations	49
	References.....	52

Figure Index

2.1	Structure and parts of a typical neuron.....	4
2.2	Changes in TP while an AP occurs	6
2.3	Graphic representation of Henneman’s Principle.....	7
2.4	Flow of electrical current between indifferent and different electrodes during NMES	8
2.5	Rectangular pulse normally used in TES	10
2.6	SDC with rheobase and chronaxie	11
2.7	Structure of superficial epidermis.....	14
2.8	Equivalent circuit model for NMES	17
2.9	Geometry and mesh of small inhomogeneities model	19
2.10	Simulation results for the small inhomogeneities model	19
3.1	Plot of the first period of Stimulation Signal 1	24
3.2	Complete geometry of the model with dis_ele = 105mm	27
3.3	Different angles of meshed geometry	29
4.1	Default result output of FEM Model	34
4.2	Comparative chart of effect of studied parameters on the uniformity of the electrical potential distribution on the gel-skin interface	37
4.3	Probabilistic distribution of the electrical potential RMS values through the gel-skin interface	38
4.4	Surface 3D graphs of the electric potential distribution	39
4.5	Comparative chart of effect of studied parameters on the uniformity of the current density distribution on the gel-skin interface	40
4.6	Probabilistic distribution of the current density RMS values through the gel-skin interface	43
4.7	Cut Line Data Set for obtaining current density RMS values	44
4.8	Current Density over the Cut Line Data Set for Signal 1-9	45
4.9	Surface 3D graphs of the current density distribution	45

4.10 Surface 3D graphs of average power dissipation	46
4.11 Comparative chart of effect of studied parameters on the uniformity of the average power dissipation on the gel-skin interface	47

Table Index

3.1	Global parameters to be used in the finite element model	23
3.2	Stimulation signal conditions implements in the model.....	23
3.3	Stimulation signal configurations for all signals.....	25
3.4	Configuration of building blocks to assemble the geometry	26
3.5	Materials electrical properties for the four different signals.....	27
3.6	Electric properties of the gel-skin interface.....	31
3.7	Time steps defined for the time dependant study	32
4.1	Probabilistic values of electrical potential throughout the gel-skin interface below the reference electrode.....	35
4.2	Probabilistic values of electrical potential throughout the gel-skin interface below the active electrode	36
4.3	Probabilistic values of current density throughout the gel-skin interface below the reference electrode	41
4.4	Probabilistic values of current density throughout the gel-skin interface below the active electrode	42
4.5	Average power dissipation throughout the electrodes	47

Chapter 1

Introduction

The Neuromuscular Electrical Stimulation (NMES) is a method used to activate nerves and muscle fibers by applying electrical current pulses using two electrodes placed on the skin. A conductive electrolyte (gel) is applied between the electrodes and the skin to obtain lower contact impedance and prevent skin damage. The current intensity used is slightly beyond the motion threshold, provoking visible muscle contractions. NMES has potential to serve as strength training, rehabilitation and post-exercise recovery tool. Previous studies have discovered that only about 20% of the applied voltage is dropped in the tissues, the rest is could be attributed to the electrode-electrolyte (gel)-skin interfaces, giving an idea of the importance of the study of these layers. A deeper understanding of the phenomena taking place in these interfaces is necessary to take full advantage of the therapeutic and diagnostic applications of the nerve stimulation technologies.

Unfortunately, the measurement of the electrical properties of the tissues presents several issues, such as the inhomogeneity of human skin, the anisotropy of muscle fibers and the non-linear phenomena of human skin. These facts make the electrical properties of the skin vary depending on the frequency and current density of the signal used for stimulation. In an effort to facilitate the studies of the NMES process, precise equivalent circuit (EC) models have been developed, including all the regions from the transcutaneous electrodes to the neuron cell membrane and then compared the experimentally obtained voltage response across the transcutaneous electrodes. In these models, the interface between the electrolyte gel and the human skin is commonly

represented by a resistance and a capacitance in parallel; however, these parameters cannot be measured unless *ex vivo* experiments are performed, resulting in unnatural measurements due to the conditions of the experiment, therefore not accounting for the full impact of this interface in current distribution.

A more in depth understanding of the gel-skin interface would help develop a more accurate model to promote more scientific advances in NMES. A simulation study of this interface, using the finite element method (FEM), would provide a comprehensive understanding of its electrical properties due to its capability to analyze complex geometries (e.g. human skin). Using FEM, a more detailed voltage and current distribution across the gel-skin interface can be obtained. Based on previous data of experimental neuromuscular electrical stimulation gathered from the literature, this Master's Thesis proposes the use of FEM software COMSOL to develop and analyze a model that will properly simulate the electrical behavior of the gel-skin interface when applying different biphasic rectangular waveform conditions, i.e. varying pulse width and amplitude of applied current.

1.1. Objectives

1.1.1.General Objective

Design a 3D geometric model that enables the proper simulation of the electrical behavior of the gel-skin interface under different rectangular signal conditions

1.1.2.Specific Objectives

- Create a model capable of assisting the further study of neuromuscular electric stimulation
- Simulate the voltage and current distribution across the gel-skin interface with an applied biphasic rectangular waveform with current intensities ranging from 14.19 to 52.89 mA
- Determine the gel-skin interface and signal conditions that accomplish the most even distribution of voltage and current throughout the area of the electrode.

1.2. Structure of the Thesis

This thesis is composed by 5 chapters. The current chapter presents an introduction to the area of study, problem description and a brief description of the proposed solution. The next chapter will provide theoretical information that might be needed for the understanding of the whole thesis such as neuromuscular system physiology, electric stimulation methods, electrical properties of materials; currently developed models to simulate electrical behavior of tissues are also described. Chapter 3 provides a description of the developed model for finite element simulation, including features, geometry, parameters, boundary conditions, and performed studies. Chapter 4 discloses the obtained simulation results and analysis of the implications of these results; and Chapter 5 lists a series of conclusions and recommendations for further research.

Chapter 2

Theoretical Background

This chapter provides the needed theoretical information during the development of the thesis. Initially, anatomical and physiological information of the nervous system is resumed, where the mechanisms of muscle activation will be described. Afterwards, an introduction to Electrical Stimulation (ES) is given, where the main focus is NMES. Subsequently, the electrical properties of the tissues involved in the NMES process will be described. Finally, a description of the FEM software COMSOL will be introduced, focusing on the Electric Currents Study, which is the most suited for the present problem.

2.1 Neuromuscular System

2.1.1 Nerve Fiber Electrophysiology

The neuron is the primary electrically excitable cell for processing and transmitting electrochemical information through the nervous system. The

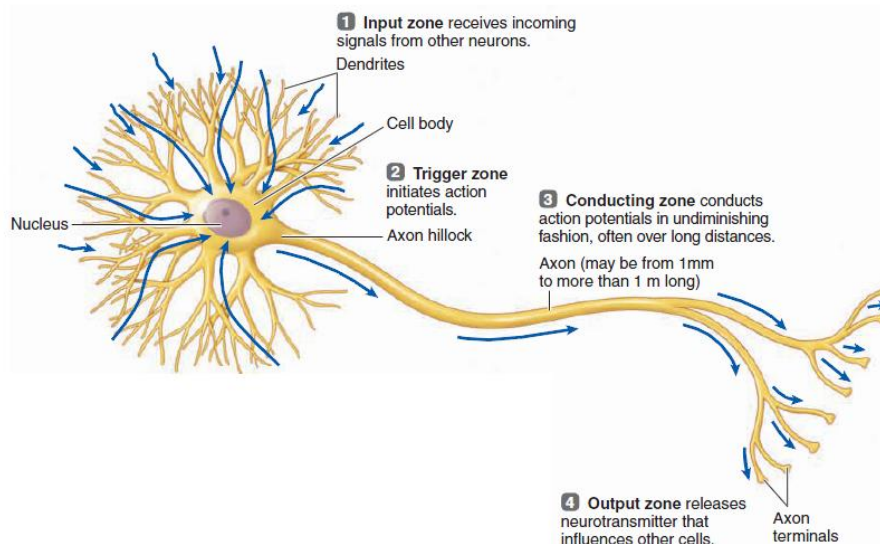


Figure 2.1: Structure and parts of a typical neuron [1]

neuron is composed of three major regions: cell body (soma), dendrites and axon (nerve fiber) (Fig. 2.1). The cell body or soma is the main body of the neuron, containing the nucleus and organelles. Numerous branches project out from the soma acting as an antenna to increase the area available for receiving signals, these are the dendrites. Finally, the axon, or nerve fiber, is an elongated projection responsible for the transmission of signals away from the cell body and eventually activating another cell or fiber. If the neuron is a motor neuron, the signal transmits from the central nervous system to the muscle fiber (efferent nerve fiber); if it is a sensory neuron, the signal is transmitted from the sensory system to the central nervous system (afferent nerve fiber). The neuron is surrounded by a membrane whose main function is to control the passage of substances into and out of the cell, including ions. A transmembrane potential (TP: electrical potential difference caused by the separation of positive and negative charges near the membrane) is always present in the cell. When the neuron is resting (not producing electrical signals), this TP is between -60mV and -90mV (typically -70mV) and is called the resting potential (RP). This charge of the cell is related to an uneven distribution of sodium (Na^+) and potassium (K^+) ions on the membrane [1]. To provoke the activation and contraction of a muscle fiber, a signal called action potential (AP) needs to be triggered (Fig 2.2). To initiate the AP, the Na^+ channels of the membrane open by order of the brain, which increases the Na^+ permeability, and sodium positively charged ions enter to exponentially depolarize the membrane, which was initially at RP, until it reaches the threshold potential (typically between -50mV and -55mV). After this point, the TP abruptly changes to a positive peak potential, typically between $+30\text{mV}$ and $+40\text{mV}$, due to an explosive increase in Na^+ permeability. When the peak voltage is reached, the sodium gates close preventing the entry of further Na^+ ions and potassium gates open to let positively charged K^+ ions to come out of the cell, rapidly restoring the TP to its RP after a slight hyperpolarization phase, caused by an excess K^+ outflow when attempting to restore the balance. This process is sequentially repeated through the whole axon until it reaches the axon terminals, where they form a chemical synapse with the motor end plate called neuromuscular junction. This gives the

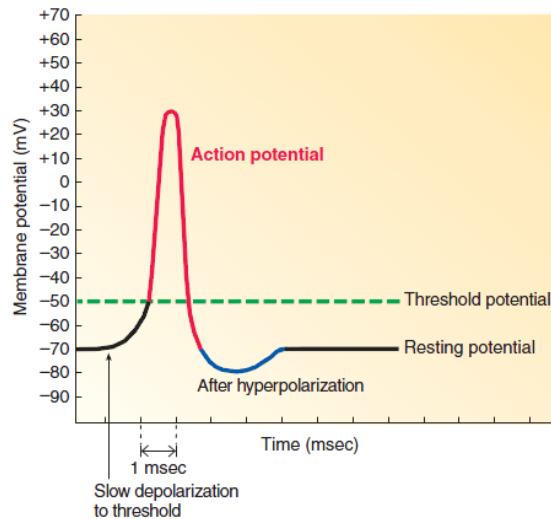


Figure 2.2: Changes in the TP while an AP occurs [1]

order of initiating an AP to the muscle fiber, which provokes its contraction.

2.1.2 Skeletal Muscle Contraction

A skeletal muscle is composed of several muscle fibers, ranging from only a few hundred to several hundred thousand. Each axon terminal of a motor neuron supplies a single muscle fiber. When the motor neuron is activated, all the muscle fibers it innervates simultaneously contract. This group of one motor neuron plus all the muscle fibers it innervates is called a motor unit. The strength of the muscle contraction is controlled by the number of motor units recruited and/or by the frequency of the contractions. Also, the innervation ratio of the motor unit plays an important role. In muscles where fine control and precision are required, like in the ocular muscles, one motor neuron controls about four muscle fibers (innervation ratio 1:4). Whereas stronger but less precise muscle, like leg muscles, reach innervation ratios of about 1:2000 [2]. Further, the motor units have a fixed order of recruitment with increasing demand of tensile strength in accordance to the Henneman's size principle [3], which states that slow and small motor units are first activated, followed in the order of increasing size to the larger and faster motor units, as shown in Fig. 2.3. Typically, the slower and smaller motor units are way more fatigue resistant than their larger counterparts, making the Henneman principle very useful to prevent early fatigue in voluntary contractions. Things are very different in

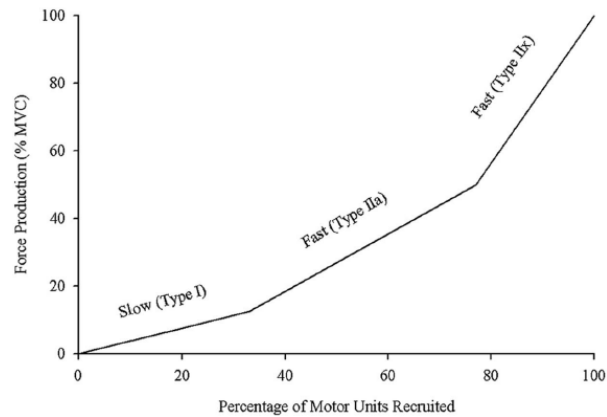


Figure 2.3: Graphic representation of the Henneman's Principle. MVC = Maximal Voluntary Contraction [4]

this manner when the contractions are elicited by electrical stimulation (ES). In the next section the different ways of applying ES are described as well as a description of the issues currently hindering the optimization of electrical stimulation systems.

2.2 Electrical Stimulation

2.2.1 Methods and Applications of Electrical Stimulation

ES is a technique used for artificial activation of nerve and muscle fibers by applying electrical current pulses to the body. The current pulse is applied between the active or different (cathode) and indifferent (anode) electrodes, causing a depolarization of the cellular membranes in excitable tissues (e.g. muscle fiber and motor and sensory neurons). ES systems can be divided in implantable, percutaneous and transcutaneous [5]. Implantable techniques make use of needle-like electrodes to provoke deep brain stimulation or cuff electrodes which are wrapped around nerves (axon) to make the stimulation as regionally specific as possible. These techniques are used for brain research [6], implanted devices for prosthesis control, treating of mental illness such as Parkinson's disease and even mood control has been demonstrated [7]–[9]. Unfortunately, the bio-compatibility of these systems when long term use is implemented is a problematic issue. Percutaneous electrical stimulation also uses needle-like electrodes but they are only slightly inserted into the skin to produce nerve activation, but infection problems may still occur. This technique

is mostly used for pain relief therapy [10], [11]. On the other hand, in transcutaneous electrical stimulation (TES) the electrodes are placed on the skin, making it possible to easily remove them after the therapy is finished, so biocompatibility and infection are no longer a problem. There are two general ways of applying TES: transcutaneous electrical nerve stimulation (TENS) and neuromuscular electrical stimulation (NMES). According to the American Physical Therapy Association, TENS is application of electrical stimulation to the skin for pain control. TENS is noninvasive, inexpensive, safe and easy to use [12]. Many variables such as pulse duration, frequency, amplitude, treatment duration and frequency have been controlled to obtain minimal to moderate pain inhibition effects in the treatment of chronic low back pain, post-stroke shoulder pain, knee osteoarthritis, acute postoperative pain, and others [13], [14]. On the other hand, NMES places a minimum of two transcutaneous electrodes on the skin, as depicted in Fig. 2.4, and uses them to apply an electrical signal with sufficiently high current intensities to elicit muscle contractions. The best sections to place the cathode are called motor points, that is where the nerves are closer to the skin surface and can be activated with minimal current intensity [5].

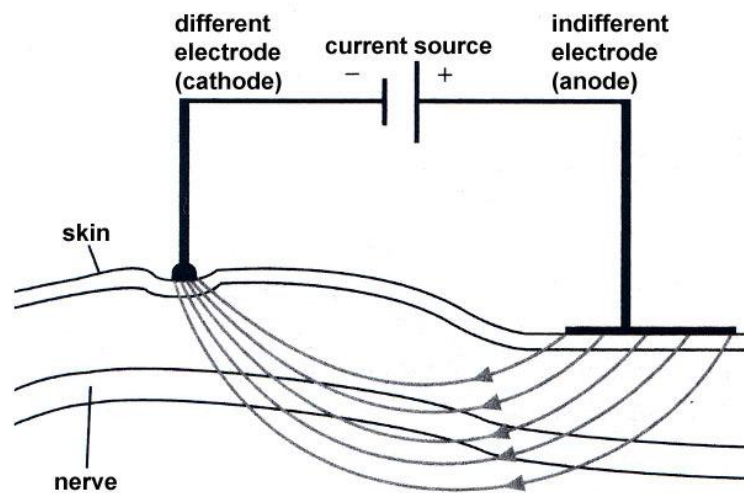


Figure 2.4: Flow of electrical current between different and indifferent electrodes during NMES [5]

This technique has received increasing attention in the last few years because it has potential to be used as strength training tool for healthy subjects and

athletes, rehabilitation and preventive tool for partially or completely immobilized patients, testing tool for evaluating the neural and/or muscular function in vivo and a post-exercise recovery tool for athletes [15]. To optimize NMES to deliver better performance in the mentioned applications, it is important to understand the mechanisms underlying the motor unit activation when applying ES, which greatly differs from the physiological way.

2.2.2 Recruitment Patterns Under NMES

In the previous section, the Henneman size principle was introduced, which dictates the order of motor unit recruitment in voluntary muscle contractions. Unfortunately, the order and mechanism of motor unit recruitment is very different when using NMES and not well known yet. It is generally accepted that a reversal of the recruitment pattern (order) is present when activating motor units with NMES. This assumption is based on two commonly agreed facts: a) motor units with higher innervation ratio are generally faster conductors of APs and have a lower resistance to electrical current [16] and b) subjects experience more fatigue when using NMES in comparison to voluntary muscle contractions [17]. Nevertheless, other investigators claim that experimental data support that ES recruits motor units in a non-selective, spatially fixed and temporarily synchronous manner [4], [18], [19]. Most experiments are performed with isometric contraction conditions, where the muscle torque is constant. If the isometric contraction is voluntary, an alternating recruitment pattern is observed, which allows for recruitment of additional motor units when the ones initially used become fatigued. However, with NMES a direct non-selective activation of the motor neurons below the electrode, regardless of size, is likely to be the case. Also, the alternating recruitment pattern does not occur in NMES, whereby the same muscle fibers are activated during the whole stimulation and some investigators attribute the increased fatigue to this situation. Accordingly, more selective and less aggressive motor unit recruitment might help to obtain better results in NMES therapy. Therefore to accomplish this goal various signal conditions and electrode distributions have been tested, but there is still much room for improvement.

2.2.3 Signal Conditions and Strength-Duration Curve

In TES, a stimulation signal is applied through the skin to artificially evoke muscle contractions. This electrical signal can be either voltage regulated or current regulated and is commonly of rectangular shape (Fig. 2.5).

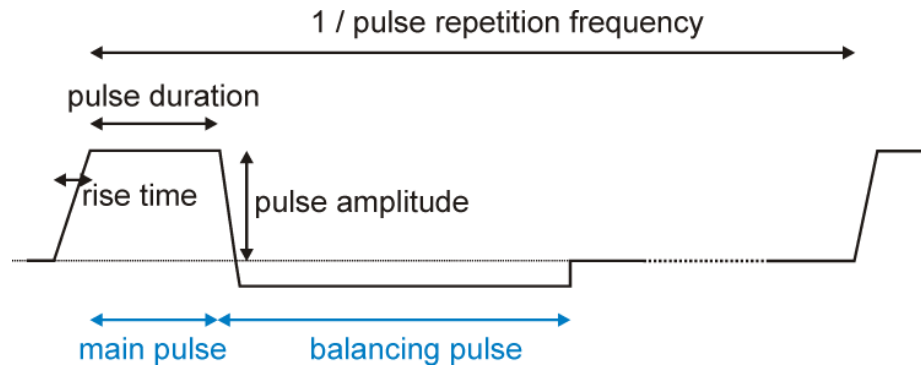


Figure 2.5: Rectangular current pulse normally used in TES [5]

These signals have a certain rise time, pulse duration, pulse amplitude, frequency and sometimes a balancing pulse can be added to reverse the modified charge distribution. The stimulation signal changes the TP of the axons under the electrodes, depolarizing under de cathode and hyperpolarizing under the anode. If the TP reaches the threshold potential for activation, an AP is generated and the muscle fiber contraction is theoretically evoked in the same way as with voluntary contraction theoretically (remember that the major problem is the non-selectiveness of the NMES process). In order to select the best signal conditions for the stimulation, an understanding of the Strength-Duration Curve (SDC) is necessary. The SDC is a plot of the least stimulus intensities required at various stimulus durations to excite a nerve [20]. In this plot, two major characteristics can be extracted a) Rheobase, the least theoretical current amplitude required to stimulate a fiber with a stimulus pulse of infinite duration and b) Chronaxie, the duration required to stimulate a fiber with a stimulus amplitude of double the rheobase [21]. In a motor nerve, the typical chronaxie is between 50 and 100 μs [22]. In Fig. 2.6, the SDC of certain fiber is plotted, where we can observe the change in the TP until it reaches the threshold potential and fires. If we focus on the red plot, it can be seen how the

threshold potential is reached rapidly due to a high amplitude current source. On the other hand, the purple plot needs more time to reach the threshold potential since it has a lower amplitude current source; the SDC resumes all this information.

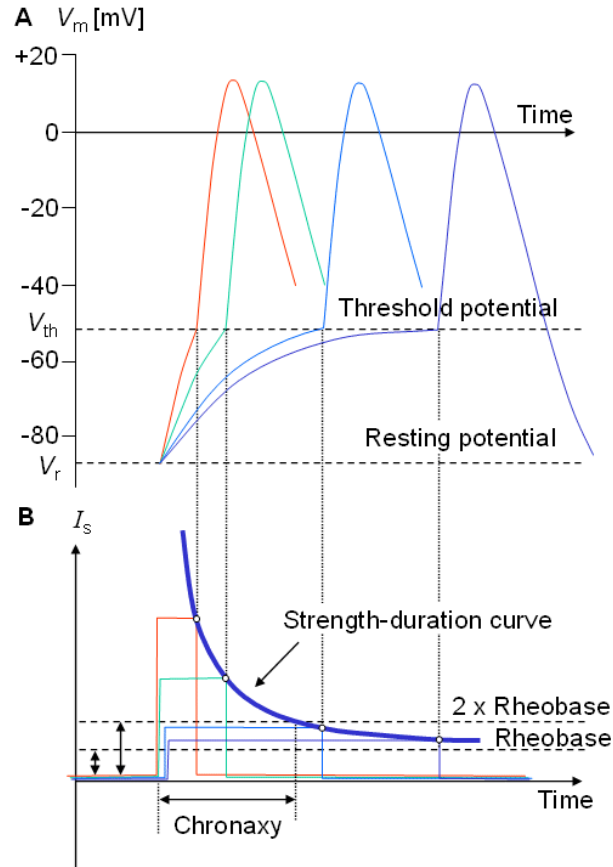


Figure 2.6: The SDC with rheobase and chronaxie [21]

Based on this fiber behavior, it can be inferred that to achieve a higher muscle recruitment percentage and consequently a stronger muscle contraction, the following actions can be taken: a) increase the pulse amplitude, b) increase the pulse duty cycle (stimulation signal ON time) and/or c) increase the pulse frequency while maintaining stimulation signal ON time. Additionally, a faster rise time would evoke more APs, because the cell would have less time to counter the change in the TP, allowing for more axons to reach the threshold potential.

2.3 Electrical Properties of Materials Involved

The electrical properties of human tissue have been of medical interest for over a century and the investigators in the field of ES are particularly interested in

them. Every material involved in the NMES has been subject of deep study everything from the electrode, going through the electrolyte, skin, fat, muscles, bones and the nerve itself. This section reviews the electrical properties that have been discovered for these materials and tissues, focusing mostly on the electrode, electrolyte and skin. The selected material properties to be introduced in the model are disclosed in Table 1 (Chapter 3).

2.3.1 Electrode and Electrolyte

This layered system is one of the most important parts to study in NMES, because contains the variables that can be changed and materials that can be engineered. Furthermore, previous studies [2] have discovered that only around 20% of the applied electric potential is dropped in the tissues, making the electrode-gel-skin interfaces a very important field of study. A good electrode-electrolyte system should be able to provide a) maximum electrode-skin contact area, where the electrode interfaces with the microscopically inhomogeneous topography of the skin in the largest area possible (liquid gel electrolytes perform the best here, being able to adapt to the irregular surface); b) homogeneous current density, applying the same current amplitude throughout the whole area of the electrode; and c) high electrode or gel impedance, which would theoretically reduce the influence of tissue electrical inhomogeneities on the spatial distribution of current [23]. Therefore, understanding the phenomena taking place here is very important for the optimization of NMES. First of all, the current is carried by electrons in electronic system, but it is carried by ions in the body, e.g. K^+ and Na^+ . The charge transfer mechanism between the different carriers takes place at the electrode-electrolyte-skin system by means of the well known redox electrochemical reaction, i.e. metal atoms M loose an electron and pass it to the electrolyte in the form of ions M^+ (oxidation), simultaneously some M^+ tend to flow towards the electrode and join a group of electrons to form a metal atom M in the electrode (reduction). This phenomenon gives rise to potentials and impedances in the electrode-electrolyte(gel) interface that can distort the stimulation signal [24]. Various electrode and gel materials have been tested to

reduce these distortions. Commonly used materials for transcutaneous electrodes are silver-silver chloride (Ag/AgCl) and carbon (C), which provide high electrical performance. These electrodes together with the appropriate gel make a contact with low level of intrinsic noise, relatively nonpolarizable and small interface impedance, but still very significant. The potential generated in this interface is called the “half-cell” potential which depends of the concentrations of ions from the electrolyte taking part in the redox reaction, temperature, materials and other variables, making it very difficult to prevent this potential from distorting the stimulation signal. The resistance to the current flow experienced by the redox reaction is termed the “charge transfer resistance” R_{CT} . Additionally, if the electrode is negatively charged with respect to the electrolyte, positively charged ions will adsorb to the electrode surface. As a consequence, there is an accumulation of equal but opposite charges in the two sides of the interface, creating an “electric double layer” and such a system behaves like a capacitor, often called “double layer capacitance” C_{DL} . At low frequencies, the impedance is dominated by R_{CT} , but as frequency increases, the capacitive impedance decreases, therefore current flows through C_{DL} , and the total impedance of the interface is reduced. In conclusion, it’s not designing a good electrode or a good electrolyte, but engineering a good interface between the two what matters to achieve a clean stimulation signal.

2.3.2 Skin

The skin is a tissue with a layered structure composed of two major layers: the dermis and the superficial epidermis. The dermis is an area of connective tissue between the superficial epidermis and the underlying subcutis, with a thickness ranging from 0.6mm for the eyelids and 3mm for the palms and soles. The dermis contains sweat glands, hair roots, nervous cells and fibers and blood vessels [25]. The epidermis is a stratified tissue made of several distinguishable layers that are composed almost entirely (95%) of keratinocytes [26], i.e. cells whose main function is providing physical and chemical protection from the exterior environment. The epidermis is mainly divided in four distinct layers: stratum basale or germinativum, stratum spinosum, stratum granulosum and

stratum corneum (SC) (Fig. 2.7). The keratinocytes are formed in the stratum basale and get surrounded by keratin (protein used for protection) and slowly ascend through the other layers until reaching the SC and eventually dying and falling off. The agglomeration of keratinized cells in the SC makes it the layer

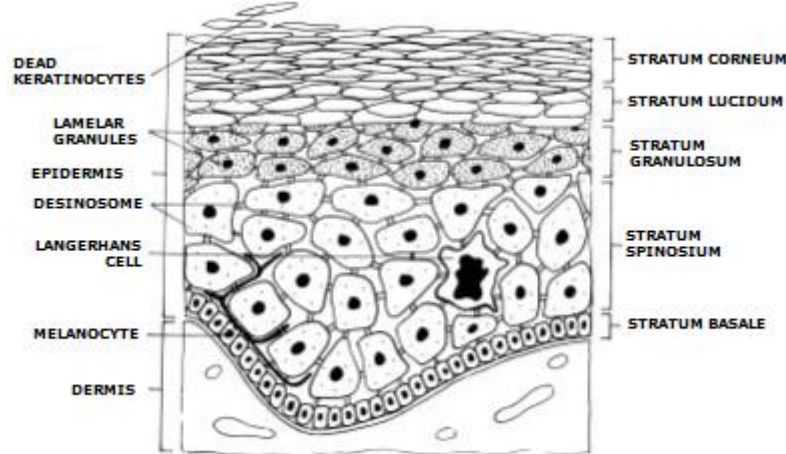


Figure 2.7: Structure of superficial epidermis [25]

with the highest impedance, almost rendering the rest negligible. This fact has been proven experimentally more than once [27]–[29], where a rapid resistance decrease is observed owing to continuous stripping of the stratum corneum with cellulose adhesive tape; when this uncomfortable process (called mild abrasion) is repeated around 15 times, the skin impedance is reduced by a factor of 100 to 1000, so it is a very common technique used to improve the contact with the electrode [30]. After the SC, all the lower layers of the skin (rest of the epidermis, dermis and subcutaneous fat) have similar and much lower electrical properties [21]. It is very important to note that the impedance of most materials, including the skin [31], is also highly dependent of the frequency and intensity of the applied signal (stimulation), which is an effect called dispersion [32]. It has been stated that the SC dominates the impedance of the skin at frequencies below 10 kHz. At low frequencies, the behavior is nearly resistive, but capacitive effects become more relevant at higher frequencies. One of the two most common equivalent circuits used to simulate this behavior is the Debye-type circuit, which is a parallel combination of a capacitor and a conductor. In this circuit, the dispersion is represented by complex-valued relative permittivity (ϵ_r^*) and conductivity (σ^*)

$$\varepsilon_r^* = \varepsilon_\infty + \frac{(\varepsilon_S - \varepsilon_\infty)}{(1 - i\omega\tau)} - i\sigma_0/\omega\varepsilon_0 \quad (2.1)$$

and

$$\sigma^* = \sigma_\infty + \frac{(\sigma_0 - \sigma_\infty)}{(1 - 1\omega\tau)} \quad (2.2)$$

where ω is the angular frequency, $\tau = 1/RC$ is the time constant, and the subscripts ∞ and S refer to frequency well above and well below the dispersion. Even though the Debye-type is a good approximation, a more precise circuit is commonly used if the dispersion is too wide spread in the material, the Cole-Cole response. This model proposes changing the conductivity and permittivity to

$$\varepsilon_r^* = \varepsilon_\infty + \frac{(\varepsilon_S - \varepsilon_\infty)}{(1 - (i\omega\tau)^\alpha)} - i\sigma_0/\omega\varepsilon_0 \quad (2.3)$$

and

$$\sigma^* = \sigma_\infty + \frac{(\sigma_0 - \sigma_\infty)}{(1 - (1\omega\tau)^\alpha)} \quad (2.4)$$

where α is a parameter that changes according to the nature of the material; it equals 1 for a Debye-type model, and decreases as the dispersion becomes wider. The equivalent circuit for this model is obtained by replacing the capacitor in the Debye-type model with a ‘‘Constant Phase Element’’ (CPE) with a complex-valued impedance of

$$Z_{CPE}^* = A(i\omega)^{-n} \quad (2.5)$$

where A is a constant and $n = \alpha$. This impedance becomes a simple resistor for $n = 0$ and a capacitive reactance for $n = 1$, allowing an ample range of materials to be modeled. Therefore, it is generally accepted when not too much precision is required, to use these circuits to represent the electrical properties of many tissues in simulation models, including the skin and the lower layers.

2.3.3 Muscles and Bones

Skeletal muscles comprise the largest group of tissues in the body, being responsible for almost half of the body's total weight [1]. As mentioned before (Section 2.1.2), a skeletal muscle is composed of several muscle fibers. These fibers are relatively large, elongated and cylinder shaped, measuring from 10 to 100 μ m in diameter and up to 2.5 feet in length (Sartorius, thinnest and longest thigh muscle). As seen with skin, muscles also have a dependency on frequency; the conductivity of the muscle dominates the impedance at low frequencies and the permittivity becomes more dominant at high frequencies [33]. Further, the muscle fibers have been categorized as highly anisotropic materials, the conduction is much easier in the longitudinal than in the transversal direction [21]. Given this peculiar property, muscle tissue must be treated differently in simulations. In finite element analysis, electrical conductivity and relative permittivity of muscle are described with a 3x3 matrix where the diagonal components contain the magnitude of these properties in the three directions.

2.4 Modeling Human Tissues

Different methods have been developed to model human tissues. A common approach is implementing an EC model like the one described in section 2.3.4. Luján et al [2] developed a precise equivalent circuit model including all the materials and tissues involved in NMES, creating a system consisting of a series of tissue "sub-systems" (Figure 2.8). This EC takes into consideration the dispersion effect of electrode-gel interface, gel-skin interface and tissues to simulate strength-duration curves obtained during experimental transdermal stimulation of the extensor muscles in the forearm of one subject. Biphasic rectangular waveform was selected as stimulation signal because it has been used as standard shape for NMES. The gel-skin interface is modeled by a resistance R_{GS} and a capacitor C_{GS} , which were adapted to match the voltage response obtained experimentally (these parameters cannot be measured unless ex vivo experiments are performed). This EC gives a fundamental understanding of the magnitudes of the different layers of human tissue involved in NMES.

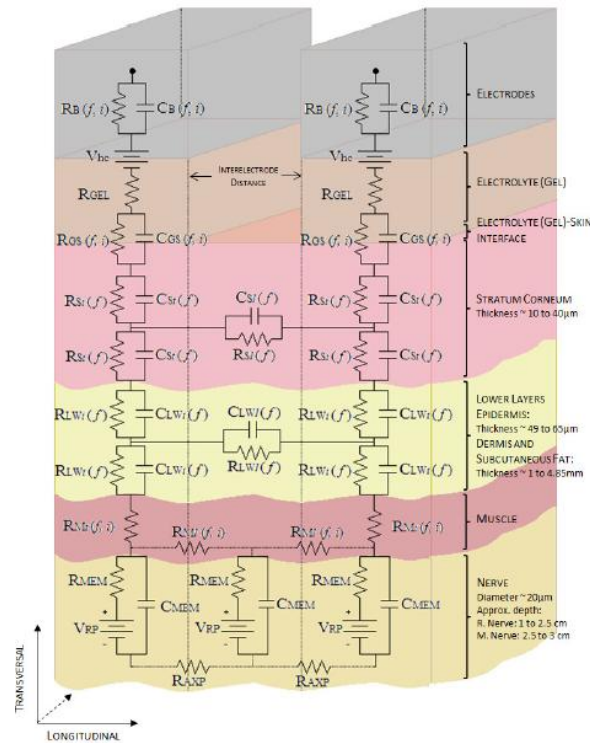
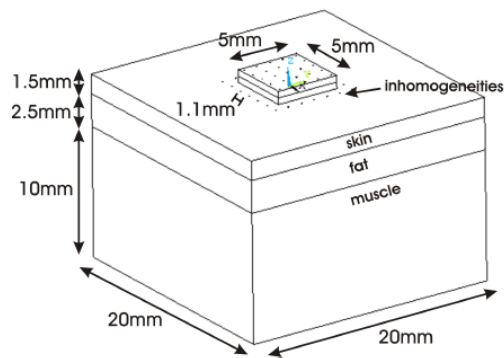


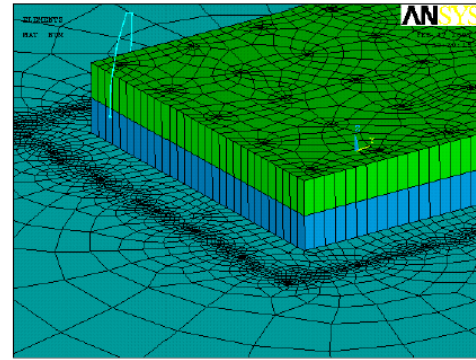
Figure 2.8. Equivalent Circuit Model for transdermal neuromuscular stimulation including all the tissue sub-systems [2]

Alternatively, in the last few years, the Finite Element Method (FEM) became a well established and convenient technique for solving complex problems in the fields of engineering and applied physics through computer simulations, since it is a powerful tool for obtaining an approximate solution of the differential equations that describe these field problems [34]. A field problem aims to obtain the spatial distribution of one or more dependent variables (structural displacement, fluid velocity, heat transfer, electric potential, etc). FEM requires a mathematical model that describes the geometry, material properties, loads and boundary conditions in terms of differential equations or integral expressions [35]. In this model, a discretization of the geometry is made, dividing the structure into a number of finite elements that are interconnected by nodes. This compound of arranged finite elements is called mesh which is represented by a series of equations that are solved for unknowns at the nodal points (these could be points where loads are applied or points where the variation of the studied field is calculated). These nodal quantities are then included in interpolation functions to determine an approximated value of the field quantity

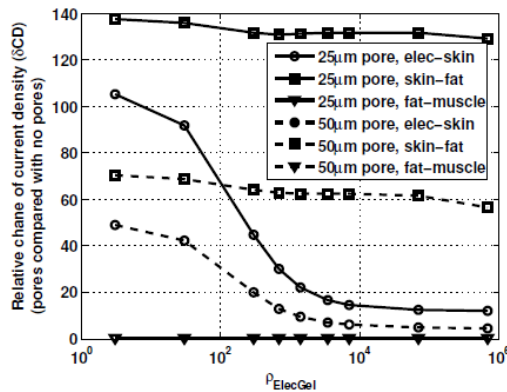
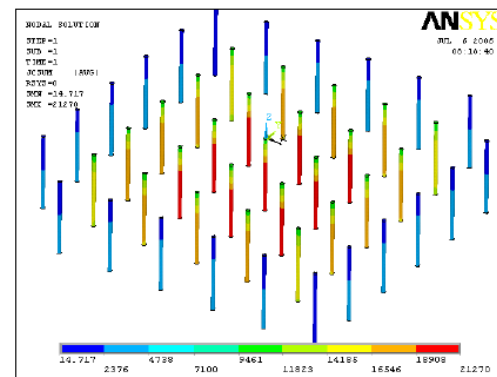
variation within each element. Finally, the field quantity is approximated in the entire structure, element by element in a piecewise fashion. This means that a FEM analysis will never obtain exact results mostly due to discretization errors (as the mesh gets coarser, the precision becomes poorer). Nevertheless, FEM offers many advantages, such as: analysis of any geometry (no matter how complex it might be), no restriction on boundary conditions or loads, different material properties can be implemented in one model and the approximation of the result can be readily improved by using smaller elements (refine the mesh) [36]. All these characteristics make FEM a desirable method for simulating spatial distribution of current in such complex geometries as the skin and other human tissues. Kuhn [5] developed a geometry to describe the potential distribution changes when the size and resistivity of the electrode is changed. The research aimed to find ways to reduce high current peaks in some areas that could cause discomfort or even skin burns. The main reasons for these high current density peaks were the fact that current densities are higher at the edges of the electrodes (Edge Effects) and also due to the inhomogeneities of the skin that lead to irregular resistance changes. An ANSYS 3D model is used to simulate the effects of small inhomogeneities within the electrode and skin in potential distribution; this is shown in Figure 2.9. These inhomogeneities represent human pores and glands that introduce new variation of resistance into the model. Figure 2.10 shows the results obtained for the current distribution. Figure 2.10 (a) shows the relative change in current density comparing a model with pores and one without pores for different electrolyte gel resistances. It can be seen how the difference in current density in the electrode-skin interface (gel) between the two models is reduced with a higher gel resistivity. Figure 2.10 (b) plots the current densities within the inhomogeneities, where it can be seen that it is higher in deeper tissues and towards the center of the electrode. Due to the aim of the research the gel-skin interface properties were not taken into account for the sake of simplicity. The mentioned models have studied the electrical properties of the human tissues, but given little importance to the gel-skin interface, which is a region where potential drops occur.



(a) Geometry with sizes.



(b) Electrode substrate and electrode gel on skin layer.

Figure 2.9. Geometry (a) and mesh (b) of the model used to analyze small inhomogeneities [5](a) Relative change of the current density δCD_i of the current density in the circles representing the inhomogeneities at the electrode/skin, the skin/fat, and the fat/muscle interface.

(b) Current density within the inhomogeneities.

Figure 2.10. Simulation results using the model with the small inhomogeneities

2.4.1 COMSOL Electric Currents Interface

In the particular case of this thesis, the FEM software COMSOL is used to determine the spatial distribution of the voltage field using the Electric Currents Interface (ECI). The ECI is within the AC/DC Module, which uses different formulations of the Maxwell Equations to describe various electromagnetic effects. Maxwell Equations are a set of four equations that describe the relationship between the electric and magnetic fields on a macroscopic level, being the foundations of classic electromagnetic theory [37], being them Gauss' Law, Gauss' Law for Magnetism, Maxwell-Faraday Law and Ampere's Law,

respectively listed:

$$\nabla \cdot \mathbf{D} = \rho \quad (2.6)$$

$$\nabla \cdot \mathbf{B} = 0 \quad (2.7)$$

$$\nabla \times \mathbf{E} = -\frac{\partial \mathbf{B}}{\partial t} \quad (2.8)$$

$$\nabla \times \mathbf{H} = \frac{\partial \mathbf{D}}{\partial t} + \mathbf{J} \quad (2.9)$$

where \mathbf{D} is the electric displacement, ρ is the charge density, \mathbf{B} is the magnetic flux density, \mathbf{E} is electric field intensity, \mathbf{H} is magnetic field intensity and \mathbf{J} is current density. The stimulation signal frequencies commonly used in NMES are below 10kHz. This means that the Maxwell equations can be used with a quasistatic approximation, in which the time-derivative of the magnetic flux density is neglected but the field components for electric field and current density are non-zero in every direction (x, y, z). This is the perfect condition for simulating electric behavior of human tissues. In this approximation the magnetic and electric fields are uncoupled, meaning that the wave propagation and inductive effects in the medium can be neglected. This consideration leaves us with a new system of equations

$$\nabla \cdot \mathbf{D} = \rho \quad (2.10)$$

$$\nabla \cdot \mathbf{B} = 0 \quad (2.11)$$

$$\nabla \times \mathbf{E} = 0 \quad (2.12)$$

$$\nabla \times \mathbf{H} = \frac{\partial \mathbf{D}}{\partial t} + \mathbf{J} \quad (2.13)$$

On the other hand, it is important to take into account the charge conservation principle which implies that electric charge can neither be created nor destroyed. This principle is defined in terms of charge density and electric current density by the equation of continuity

$$\nabla \cdot \mathbf{J} = -\frac{\partial \rho}{\partial t} \quad (2.14)$$

which states that the only way for the charge density to change in a point is for an electric current charge to flow into or out of the point. Additionally, constitutive relations that describe the reaction of materials to applied electric fields have to be taken into account

$$\mathbf{D} = \varepsilon_0 \mathbf{E} + \mathbf{P} \quad (2.15)$$

$$\mathbf{J} = \sigma \mathbf{E} \quad (2.16)$$

where \mathbf{P} is the electric polarization vector. These equations describe how the material can get electrically charged or polarized when an electric field is present. In the NMES model, ECI is used to apply a current regulated signal in the indifferent electrode and solve for the electric potential at the nodal points of the mesh and finally obtaining a graphical spatial distribution of the field. A more detailed description of the model is given in Chapter 3.

Chapter 3

Finite Element Model

The Finite Element Model further described is a three dimensional model that uses COMSOL's Electric Currents Interface with a Time Dependent Study with the purpose of calculating the spatial distribution of the current on the Gel-Skin Interface. This chapter describes the parameters and methods used to develop the finite element model. First, an introduction to the parameters used in the model is made. Then, the stimulation signal to be used will be described, as well as the way to simulate it, followed by a description of the geometry, material properties, boundary conditions, meshing and solver used in the model. Quotations marks in this Chapter will be used to denote commands, modules or nodes used within the COMSOL User's Interface to develop the model, e.g. "Rectangular Function"

3.1 Parameters

"Parameters" are expressions or values accessible in all parts of the model and they are defined on the "Global Definitions Node". For this particular model, parameters are used to define geometry dimensions, stimulation signal conditions and electrical properties. Table 3.1 summarizes all the parameters used in the model. Signal conditions were defined in the parameters to facilitate changes to the model when different signals need to be studied. Some parameters such as electrode separation distance and positive pulse duration were subject to a "Parametric Sweep", which iterates different combinations of values to determine the influence on the current spatial distribution. The electrical property parameters are based on experimental data gathered by Luján et al [2], where NMES was applied to the forearm of various subjects,

Signal Conditions		Electrical Properties	
Amp =	Stimulation Signal Amplitude (A/m ²)	c_E =	Electrode Conductivity (S/m)
Rt =	Stimulation Signal Rise Time (s)	p_E =	Electrode Relative Permittivity
Per =	Stimulation Signal Period (s)	c_GSI =	Gel-Skin Interface Conductivity (S/m)
Pd =	Stimulation Positive Pulse Duration (s)	p_GSI =	Gel-Skin Interface Relative Permittivity
Des =	Stimulation Signal Initial Continuity Time Gap (s)	c_SC =	Stratum Corneum Conductivity (S/m)
		p_SC =	Stratum Corneum Relative Permittivity
		c_LL =	Lower Layer Conductivity (S/m)
		p_LL =	Lower Layer Relative Permittivity
		c_F =	Subcutaneous Fat Conductivity (S/m)
		p_F =	Subcutaneous Fat Relative Permittivity
		c_Ml =	Longitudinal Muscle Conductivity (S/m)
		p_Ml =	Longitudinal Muscle Relative Permittivity
		c_Mt =	Transverse Muscle Conductivity (S/m)
		p_Mt =	Transverse Muscle Relative Permittivity
Geometry Dimensions			
dis_ele =	Distance between electrodes (mm)		
w_ele =	Width of the Electrodes (mm)		
l_ele =	Length of the Electrodes (mm)		
tisover =	Tissue Overlap with Electrodes (mm)		

Table 3.1. Global parameters to be used in the finite element model

therefore the developed finite element model represents the surface of the forearm, but parameters can be adjusted to simulate other parts of the body. Additionally, the literature was also reviewed to assign parameters of the model that were not measured in the experiment. The values of these parameters will be disclosed in the following corresponding sections.

3.2 Stimulation Signal

Many waveforms have been used for NMES e.g. sine, spike, square. The rectangular (square) waveform is often used because it has been proven to be relatively more comfortable for the patient [38]. Therefore, a current regulated biphasic square signal with 4 different combinations of intensities and frequencies are simulated, as described on Table 3.2, to verify the effect of these conditions on the electrical behavior of the interface. The electrodes simulated are rectangular with a cross section area of $4,5\text{cm} \times 8\text{cm} = 0.0036\text{m}^2$. These amplitudes together with the electrode sizes correspond to the range of study set

Signal	Current Intensity (A/m ²)	Period (μs)
1	± 3.9417	1024
2	± 5.7333	512
3	± 7.5250	256
4	± 14.6916	128

Table 3.2. Stimulation signal conditions implemented in the model

on the objectives (14.19 to 65.79mA). Each signal is studied on a different simulation; therefore, four separate simulations are performed. The signal condition parameters listed on the previous section are used to define:

- ***Amp***: The amplitude of the signal. The values of this parameter are listed on the second column of Table 3.2.
- ***Rt***: A transition time (the time it takes to switch states) for the signal has to be included to give the design continuity, which is extremely necessary on FEM. If abrupt changes happen the solver will not be able to provide the correct estimations, crashing the simulation. A transition time of $2\mu\text{s}$ is used for every signal.
- ***Per***: Period of the stimulation signal. The designated values are listed on Table 3.2
- ***Pd***: It has been observed that the pulse duration also has an effect on the electrical behavior of tissues; therefore, a “Parametric Sweep” is done to simulate three different cases of positive pulse duration: 30%, 50% and 70% of the signal period ($Pd = \{0.3*Per, 0.5*Per, 0.7*Per\}$)
- ***Des***: To avoid problems that might arise with the initial values of the model, an initial time gap is defined in which the signal is at 0V. This value is $15\mu\text{s}$ for all signals.

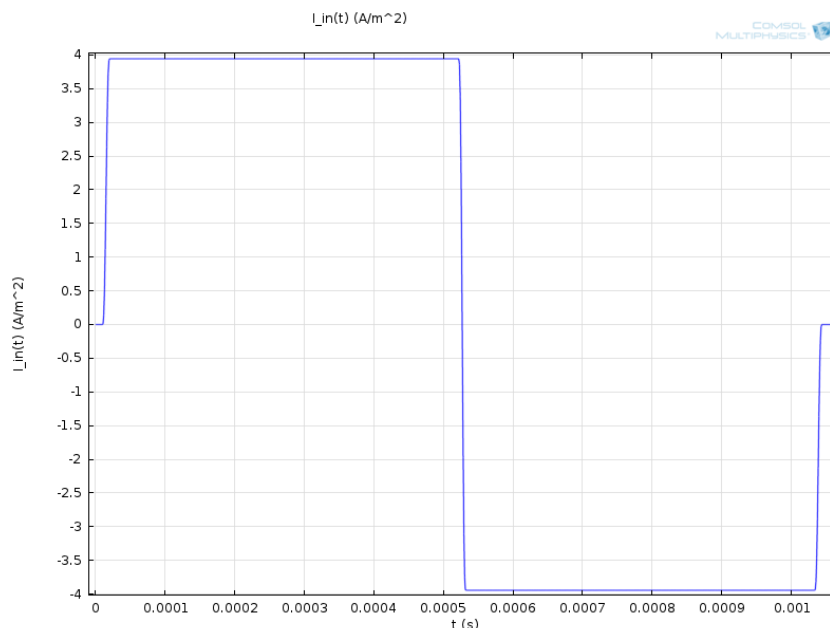


Figure 3.1. Plot of the first period of Stimulation Signal 1

Signal 1 is plotted in Fig. 3.1. To implement these signals two “Rectangle Function” from the “Definitions Branch” were used; one for positive pulse and other for negative pulse (these functions determine the pulse durations). These two functions were then introduced into an “Analytic Function”, where they were added together. In this function, the amplitude and the physical unit of the signal are specified. This “Analytic Function” represents the stimulation signal and will be the input current density of the model. The configuration of the functions in COMSOL is resumed on Table 3.3.

Rectangle Function 1			Rectangle Function 2		
Section	Field	Value	Section	Field	Value
Function Name	Function Name	rect1	Function Name	Function Name	rect2
Parameters	Lower Limit	Des	Parameters	Lower Limit	Pd + Des
	Upper Limit	Pd + Des		Upper Limit	Per + Des
Smoothing	Size of transition zone	Rt	Smoothing	Size of transition zone	Rt

Analytic Function 1		
Section	Field	Value
Function Name	Function Name	I_in
Definition	Expression	Amp*(mod1.rect1(t)-mod1.rect2(t))
	Arguments	T
Units	Arguments	S
	Function	A/m^2

Table 3.3. Stimulation signal configuration for all signals

3.3 Geometry

The whole geometry is defined in mm. For the sake of saving computational power and simplicity, the geometry is based solely on blocks. The complete geometry consists of a total of six “Blocks” and a “Copy Transform”, representing areas of material or tissue from the electrode to the muscle. Simulations were made taking into account bone material, but no significant changes were observed on the spatial distribution of current density in the Gel-Skin Interface. A few parameters were defined to facilitate the customization of the original geometry:

- *dis_ele*: The distance between the electrodes is also included in the

“Parametric Sweep” to determine which distance achieves a better spatial distribution of the current density. Three values are studied: 85mm, 105mm and 125mm.

- w_{ele} : Width of the electrodes are set to be the same as the ones used by Luján [2] (45mm) to provide a better agreement with the material properties used in the model.
- l_{ele} : The same case as the width of the electrodes. The length is set to 80mm
- $tisover$: This parameter refers to the amount of coverage the tissue has over the electrode, i.e. the length from the edge of the gel block to the edge of the stratum corneum block and is set to 15mm.

Table 3.4 summarizes the configuration of the six blocks. To simplify the table, the following formulas are defined:

$$S = 2 * (w_{ele} + tisover) + dis_{ele} \quad (3.1)$$

$$T = 2 * tisover + l_{ele} \quad (3.2)$$

$$U = -(w_{ele} + tisover + dis_{ele}) \quad (3.3)$$

Section	Field	<i>blk1</i>	<i>blk2</i>	<i>blk3</i>	<i>blk4</i>	<i>blk5</i>	<i>blk6</i>
Name		Electrode	Gel	Stratum Corneum	Lower Layers	Fat	Muscle
Size and Shape	Width	w_{ele}	w_{ele}	S^*	S^*	S^*	S^*
	Depth	l_{ele}	l_{ele}	T^*	T^*	T^*	T^*
	Height	1	1	0.04	1.5	2.5	20
Position	x	0	0	U^*	U^*	U^*	U^*
	y	0	0	$-tisover$	$-tisover$	$-tisover$	$-tisover$
	z	1	0	-0.04	-1.54	-4.04	-24.04

Table 3.4. Configuration of building blocks to assemble the geometry

*These variables are defined on (3.1-3)

The “Copy Transform” is used to build the second electrode-gel group (different electrode) by selecting *blk1* and *blk2* as “Input Objects” and setting the x field under the “Displacement Section” to $-(dis_{ele}+w_{ele})$. The completely built geometry is shown on Figure 3.2.

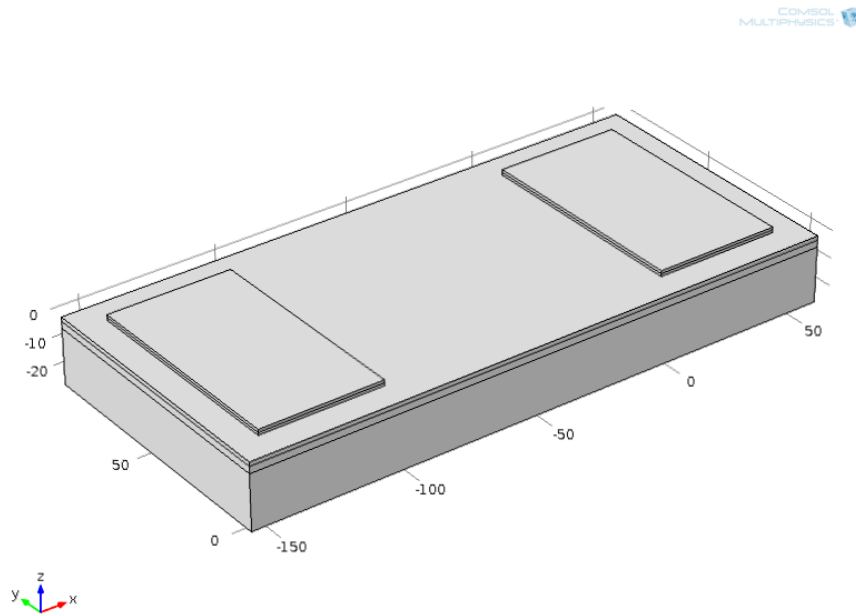


Figure 3.2. Complete geometry of the model with $dis_ele = 105\text{mm}$

3.4 Materials

A total of six custom materials were created (Electrode, Gel, Stratum Corneum, Skin Lower Layers, Subcutaneous Fat and Muscle) to specify the electrical

Parameter	Signal 1*	Signal 2*	Signal 3*	Signal 4*
c_E	1.70×10^{-2}	2.10×10^{-2}	2.13×10^{-2}	2.03×10^{-2}
p_E	1.18×10^4	1×10^4	7.76×10^3	9.06×10^3
c_G	5.24×10^{-3}	5.24×10^{-3}	5.24×10^{-3}	5.24×10^{-3}
p_G	1	1	1	1
c_SC	2.70×10^{-5}	6×10^{-5}	8×10^{-5}	1.4×10^{-4}
p_SC	2×10^3	2×10^3	1.90×10^3	1.42×10^3
c_LL	0.2	0.2	0.2	0.2
p_LL	2.20×10^5	1.80×10^5	1.40×10^5	1.10×10^5
c_F	3.10×10^{-2}	3.10×10^{-2}	3.10×10^{-2}	3.10×10^{-2}
p_F	3×10^4	3×10^4	3×10^4	3×10^4
c_MI	0.24	0.25	0.3	0.34
p_MI	2×10^5	2×10^5	2×10^5	2×10^5
c_Mt	0.12	0.12	0.157	0.158
p_Mt	8×10^4	8×10^4	8×10^4	8×10^4

Table 3.5. Material electrical properties for the four different signal conditions. Values obtained from experimental data and literature [2], [5], [31]. * Stimulation signal characteristics are specified on Table 3.2

properties of all the materials involved. Each material is assigned to the corresponding block of the geometry and assigned the corresponding conductivity and relative permittivity parameters. As explained in Chapter 2, these values are frequency and current density dependant; therefore each signal requires different values of electrical properties for the materials. The values selected for the parameters introduced on Table 3.1 are disclosed on Table 3.5.

3.5 Meshing

Due to the incredible difference in the geometry dimensions, a custom mesh had to be made based on “Swept”, “Free Triangular” and “Edge” nodes. The regions of the model that require smaller elements are those close to the Gel-Skin Interface and the edge of the gel blocks, because the rest of the geometry is relatively uniform. The sequence for the meshing consists of two “Edge”, one “Free Triangular”, one “Swept” and one “Free Tetrahedral” node. The “Distribution” and “Size” nodes are used to define the number of elements and their proper arrangement. Experimental stationary simulations were carried out to determine the best balance between precision and computational power; progressively smaller elements (finer meshing) were used for the mesh until no significant change in the results were observed. The values further mentioned are the ones that achieve this balance. By default, a general “Size” node is the first one in the Geometry sequence and will provide the guidelines for the sizing of all the elements in the mesh; the option “Custom” is selected to manually set some element size parameters. The “Maximum element size” is set to 9mm and the “Maximum element growth rate” is set to 1.2; this node will prevent the elements that are farther from the electrode to get excessively big, which would be detrimental for precision. The two “Edge” nodes were applied on the bottom edges of the gel blocks (blk2 and the corresponding copy). One node is applied to the shorter edges (45mm) and the other to the longer edges (80mm). A “Distribution” node is created under both “Edge” nodes for the purpose of specifying the “Number of Elements” these that will be used for this portion of the mesh, setting this field to 85 elements for the shorter edges and 150 for the longer edges. Following with the sequence, the “Free Triangular” node is created,

applying it to the three boundaries that comprise the top face of the Stratum Corneum, no further customization is necessary for this node; the general “Size” node will provide the appropriate characteristics. The “Free Triangular” mesh will serve as source for the “Swept” node, which is a specialized meshing tool for thin geometries which takes the mesh of a source face and sweeps it through the specified domain onto the opposite destination face, creating column like elements connecting both faces. For this node, the selected domains are the Stratum Corneum and the Lower Layers blocks, the source faces are the boundaries comprising the top area of the Stratum Corneum and the destination face is the boundary between the Lower Layers and Fat. A “Distribution” node is created for “Swept” and the “Number of elements” field is set to 1; setting a higher number in this field would decrease the quality of the elements on the Stratum Corneum and Lower Layers domains. Finally, a “Free Tetrahedral”

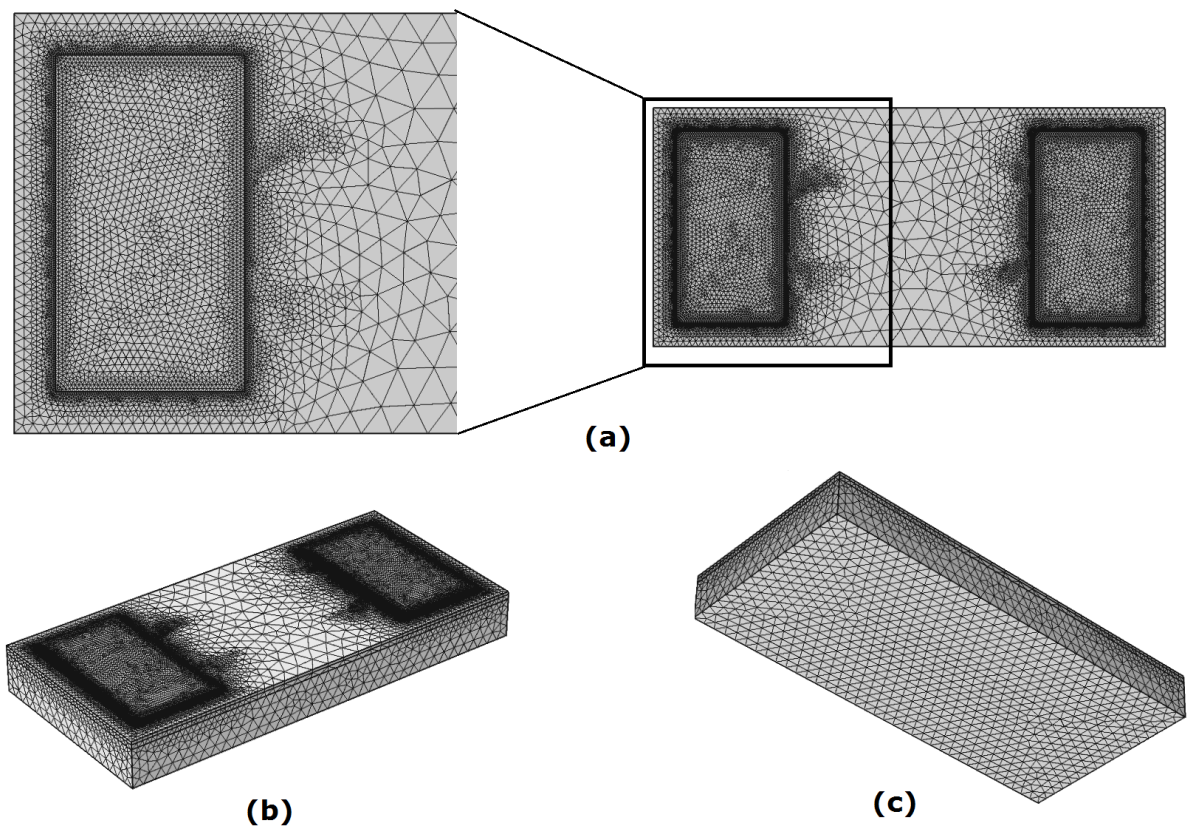


Figure 3.3. Different angles of the meshed geometry a) Top view with a close-up of the different electrode b) Isometric view c) bottom view

node is included and is set to mesh the remaining domains: electrode, gel, fat and muscle. The complete mesh consists of a little over 200.000 elements and different views of the same are shown on Figure 3.3

3.6 Boundary Conditions

The boundary conditions (BC) are defined to describe how the Maxwell Equations and constitutive relations introduced in the previous chapter will interact with the material properties and geometry of the model. There are three default nodes in the “Electric Currents (ec)” sequence:

- **Current Conservation:** This is a property applicable to complete domains which adds the continuity equation and constitutive relations for electric potential and provides an interface for introducing electric conductivity and relative permittivity for the displacement current. Every domain in the model is included in this node as a default condition.
- **Electric Insulation:** This BC is applied by default to every external boundary and it prevents electric current to flow into the boundary, that means $\mathbf{n} \cdot \mathbf{J} = 0$ is applied. The top boundaries of the electrode blocks will get overridden by latter boundary conditions that don't obey the mentioned equation.
- **Initial Values:** All the domains are selected for this node also and it specifies the initial magnitude of the electric potential in selected domains. Human tissues possess a resting potential in the range of mV which is negligible compared to the magnitude of tens of volts that are observed on the tissues due to the stimulation signal; therefore the initial value for every domain is left as default: 0V.

Apart from the default nodes, other three boundary conditions were added to determine the input/output of the stimulation signal and describe the electric properties of the Gel-Skin Interface:

- **Normal Current Density:** This BC is applicable to external boundaries that represent either a source or sink of current. In this case it represents the input of the stimulation signal (source) representing the normal current density as the inward current flow

$$-\mathbf{n} \cdot \mathbf{J} = J_n \quad (3.4)$$

Where J_n is the stimulation signal created as described on section 3.2; therefore, the “Normal Current Density” field is set to *mod1.I_in(t)*. Logically, this BC is applied to the top of the indifferent electrode block (right electrode, picked arbitrarily, the electrode in the model are interchangeable)

- **Ground:** BC in which the electric potential is set to zero ($V=0$). This is the area of outflow of current from the model and the top boundary of the different electrode is selected (left electrode).
- **Contact Impedance:** This BC is used to model thin layers of material on interior boundaries, which makes it perfect to simulate the electric properties of the Gel-Skin Interface. The two boundaries between the electrode and gel blocks are selected. On the “Surface thickness” field, the value 0.03[mm] is set. Subsequently, both the electric conductivity and relative permittivity fields are set to user defined and the values c_GSI and p_GSI respectively; according to Table 3.6. These values are defined in the Parameters node described at the beginning of the chapter. These values were calculated by Luján et al as a result of the NMES experiments performed on the forearm.

Parameter	Signal 1	Signal 2	Signal 3	Signal 4
c_GSI	4.62E-05	4.84E-05	1.31E-04	5.36E-04
p_GSI	1.44E+04	1.18E+04	1.11E+04	1.03E+04

Table 3.6. Electric properties of the Gel-Skin Interface for the four different signal conditions

3.7 Study and Solver Configuration

In the “Study” node is where the “Parametric Sweep” for the parameters *dis_ele* and *Pd* is configured, which prepares the software to run the simulation sequence as many times as needed to study all the variations of parameters specified. “Sweep Type” is set to All Combinations so every possible combination

of *dis_ele* and *Pd* is studied. In the “Study Settings” table the first parameter is *dis_ele* with values set to 85, 105, 125; in the second row is *Pd* with the values set to 0.3*Per, 0.5*Per, 0.7*Per. Arranging them in this order will take advantage of the “Parametric Solver” which takes the results of one simulation sequence to make approximations of the results for the next one as long as the degrees of freedom don’t change, reducing the needed computation time. Following with the “Time Dependent” node, only the first period of the stimulation signal is studied. The values for the time steps are set so that the calculations are done 20 times through the signal, as resumed on the Table 3.7. For every simulation the “Direct” attribute is enabled for the “Time Dependent Solver”. Doing so selects MUMPS as the linear solver for the calculation of the spatial distribution of electric potential, which benefits from shared memory parallelism. The PC used for the simulations runs on two 2.93GHz Intel Xeon processors so the Direct solver can take advantage of both of them.

Signal	Start	Step	Stop
1	0	0.00005275	0.001055
2	0	0.000027	0.00054
3	0	0.000014	0.00028
4	0	0.0000075	0.00015

Table 3.7. Time steps defined for the time dependant study

In the next chapter, the obtained results for the four simulations are shown and also the performed analysis of these results will be disclosed.

Chapter 4

Results and Analysis

The model described on Chapter 3 provides as default output the instantaneous electrical potential of 20 time steps along the first period of the biphasic stimulation signal. This electrical potential is calculated all around the geometry using as input the parameters disclosed on the previous chapter, resulting in a spatial distribution of the electrical potential, which can be used for calculating other electrical variables such as current density and power consumption. The analysis of these results is made on this chapter, providing valuable information to study the electrical behavior of the Gel-Skin interface.

4.1 Electrical Potential Distribution

The default output of the model consists of a 3D multislice plot of the electrical potential distribution throughout the entire geometry, generating a group of data for every time step. In Fig 4.1 there is an example showing the instantaneous electrical potential distribution obtained for Signal 1 with a positive pulse duration (Pd) of 50% of the period and an electrode separation distance of $dis_ele=125\text{mm}$ at $t=2.64 \times 10^{-4}$ seconds. It can be seen how the greatest amount of voltage drop occurs on the reference (indifferent) electrode. For the sake of focusing on the gel-skin interface two Surface “Data Sets” were defined under the Results node, setting the surface between the gel of the reference (Surface 1) and active (Surface 2) electrodes and the Stratum Corneum as selection. These Data Sets select only the values of instantaneous electrical potential calculated by COMSOL on the nodes that sit on the surfaces (both Gel-Skin Interfaces). The data of the Surface Data Sets were added to the

“Export” node and exported the values on a spreadsheet format that could be processed on Microsoft Office Excel® to obtain the RMS value for every point node in the surface using

$$V_{RMS} = \sqrt{\frac{1}{n} \sum_{i=1}^n V_i^2} \quad (4.1)$$

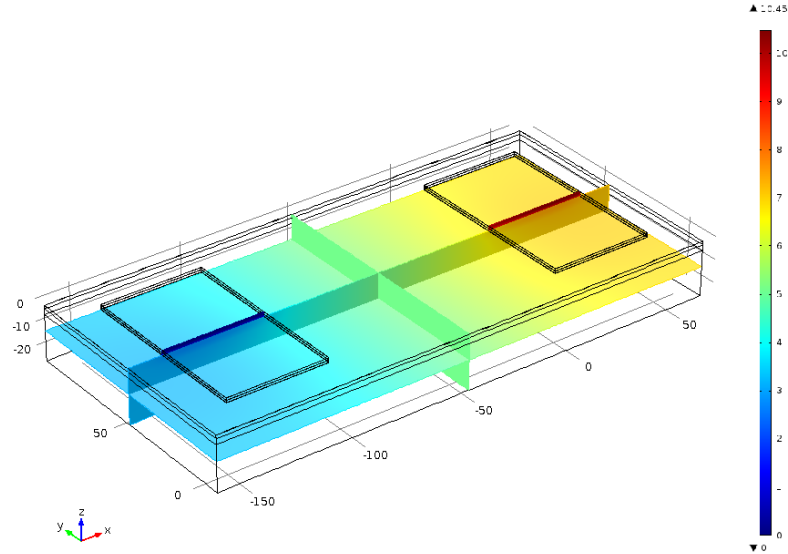


Fig. 4.1. Example of default result output for the model. Multislice plot of the electrical potential distribution for signal 1 with electrode separation of 105mm ($dis_ele=105mm$) and a positive pulse duration (Pd) of 50% of the signal period ($Pd = 0.5$) at $t = 2.64 \times 10^{-4}$

Using the RMS values, the mean and standard deviation were calculated, obtaining the values shown on Table 4.1 (Reference Electrode) and Table 4.2 (Active Electrode), where \bar{X} is the arithmetic mean of the RMS voltage throughout the surface between the gel of the electrodes and the stratum corneum in the model, σ is the standard deviation and $\sigma (\%)$ is the standard deviation expressed in percentages. These values can be used as a way to measure the uniformity of the electrical potential distribution on the gel-skin interfaces; if the standard deviation is higher, the values are more disperse apart, making the distribution less uniform. The graph in Fig 4.2 shows a comparison of the standard deviation of the electric potential distribution for various cases depending on electrode separation distance, Pd (duration of the positive portion of the biphasic stimulation signal) and amplitude of the signal.

Signal ID	Signal Amplitude (A/m ²)	Electrode Separation (mm)	Pd	\bar{X} (V)	σ (V)	σ (%)	Range (V)
1-1	±3.9417	85	30%	7.39707	± 0.21148	2.86%	1.11948
1-2			50%	6.89309	± 0.20073	2.91%	1.06034
1-3			70%	8.09133	± 0.18491	2.29%	1.09855
1-4		105	30%	7.84781	± 0.21418	2.73%	1.14475
1-5			50%	7.32168	± 0.20449	2.79%	1.08719
1-6			70%	8.47574	± 0.18927	2.23%	1.13217
1-7		125	30%	8.29057	± 0.21625	2.61%	1.13992
1-8			50%	7.75021	± 0.20772	2.68%	1.08641
1-9			70%	8.86492	± 0.19295	2.18%	1.12725
2-1	±5.7333	85	30%	6.30978	± 0.22707	3.60%	1.11685
2-2			50%	5.90149	± 0.23265	3.94%	1.09899
2-3			70%	6.41151	± 0.22898	3.57%	1.13043
2-4		105	30%	6.78148	± 0.23070	3.40%	1.13980
2-5			50%	6.38719	± 0.23487	3.68%	1.11605
2-6			70%	6.89208	± 0.23166	3.36%	1.15054
2-7		125	30%	7.29283	± 0.23426	3.21%	1.14501
2-8			50%	6.88079	± 0.23656	3.44%	1.11589
2-9			70%	7.37178	± 0.23346	3.17%	1.14806
3-1	±7.5250	85	30%	8.20611	± 0.35115	4.28%	1.65079
3-2			50%	7.94126	± 0.35339	4.45%	1.63884
3-3			70%	8.39310	± 0.34095	4.06%	1.63949
3-4		105	30%	8.90601	± 0.35234	3.96%	1.66571
3-5			50%	8.65979	± 0.35496	4.10%	1.65591
3-6			70%	9.07508	± 0.34351	3.79%	1.65984
3-7		125	30%	9.60610	± 0.35302	3.67%	1.66195
3-8			50%	9.36428	± 0.35619	3.80%	1.65454
3-9			70%	9.76318	± 0.34558	3.54%	1.65891
4-1	±14.6916	85	30%	13.84526	± 0.61055	4.41%	2.89161
4-2			50%	13.15603	± 0.60046	4.56%	2.81582
4-3			70%	13.76606	± 0.60046	4.36%	2.86751
4-4		105	30%	14.96555	± 0.61153	4.09%	2.90536
4-5			50%	14.31022	± 0.60234	4.21%	2.83678
4-6			70%	14.92378	± 0.60289	4.04%	2.89366
4-7		125	30%	16.18508	± 0.61222	3.78%	2.90502
4-8			50%	15.46462	± 0.60344	3.90%	2.83343
4-9			70%	16.08677	± 0.60498	3.76%	2.89126

Table 4.1. Arithmetic mean (\bar{X}) and standard deviation (σ) of the electrical potential throughout the gel-skin interface located below the reference electrode. Positive pulse duration expressed in percentage of time of the signal period.

Signal ID	Signal Amplitude (A/m ²)	Electrode Separation (mm)	Pd	\bar{X} (V)	σ (V)	σ (%)	Range (V)
1-1	±3.9417	85	30%	1.08123	± 0.10075	9.32%	0.72561
1-2			50%	1.01884	± 0.09493	9.32%	0.65695
1-3			70%	1.07732	± 0.10302	9.56%	0.75214
1-4		105	30%	1.08133	± 0.10086	9.33%	0.72759
1-5			50%	1.01869	± 0.09464	9.29%	0.65797
1-6			70%	1.07765	± 0.10319	9.58%	0.75218
1-7		125	30%	1.08206	± 0.10207	9.43%	0.73667
1-8			50%	1.01916	± 0.09548	9.37%	0.66536
1-9			70%	1.07766	± 0.10354	9.61%	0.75920
2-1	±5.7333	85	30%	1.04448	± 0.12790	12.25%	0.78491
2-2			50%	1.02663	± 0.12940	12.60%	0.76396
2-3			70%	1.06509	± 0.12782	12.00%	0.80055
2-4		105	30%	1.04597	± 0.13007	12.44%	0.79564
2-5			50%	1.02695	± 0.12978	12.64%	0.76842
2-6			70%	1.06492	± 0.12755	11.98%	0.80209
2-7		125	30%	1.04723	± 0.13135	12.54%	0.80511
2-8			50%	1.02687	± 0.12975	12.64%	0.77120
2-9			70%	1.06494	± 0.12780	12.00%	0.80621
3-1	±7.5250	85	30%	1.88083	± 0.23453	12.47%	1.28202
3-2			50%	1.87634	± 0.24511	13.06%	1.30556
3-3			70%	1.86065	± 0.23020	12.37%	1.26038
3-4		105	30%	1.88115	± 0.23475	12.48%	1.28873
3-5			50%	1.87573	± 0.24373	12.99%	1.30958
3-6			70%	1.86082	± 0.23030	12.38%	1.26658
3-7		125	30%	1.88109	± 0.23507	12.50%	1.29240
3-8			50%	1.87586	± 0.24430	13.02%	1.31329
3-9			70%	1.86116	± 0.23079	12.40%	1.27114
4-1	±14.6916	85	30%	3.59158	± 0.43525	12.12%	2.34728
4-2			50%	3.55465	± 0.43877	12.34%	2.30576
4-3			70%	3.49734	± 0.42357	12.11%	2.27342
4-4		105	30%	3.59186	± 0.43733	12.18%	2.36071
4-5			50%	3.55597	± 0.43958	12.36%	2.32029
4-6			70%	3.49838	± 0.42381	12.11%	2.28580
4-7		125	30%	3.59122	± 0.43610	12.14%	2.36428
4-8			50%	3.55559	± 0.44040	12.39%	2.32565
4-9			70%	3.49928	± 0.42487	12.14%	2.29392

Table 4.2. Arithmetic mean (\bar{X}) and standard deviation (σ) of the electrical potential throughout the gel-skin interface located below the active electrode. Positive pulse duration expressed in percentage of time of the signal period.

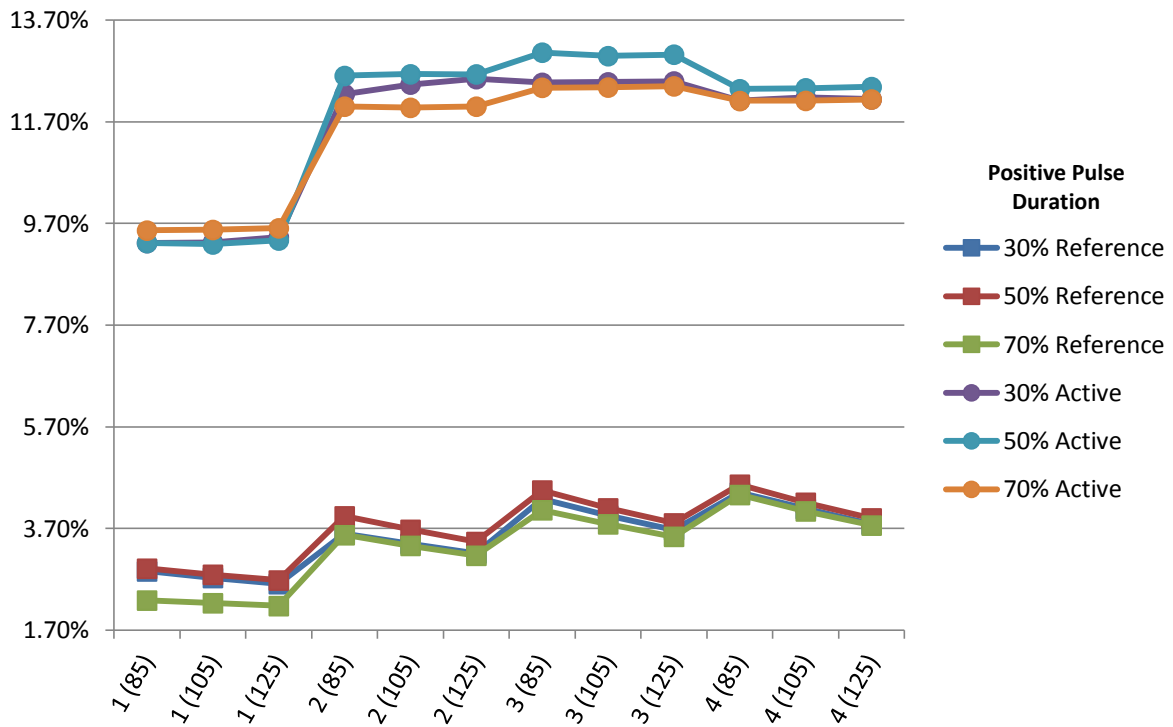
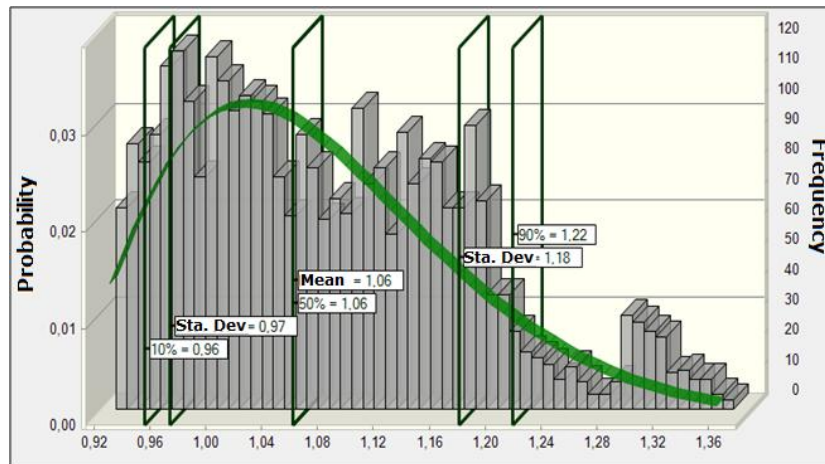


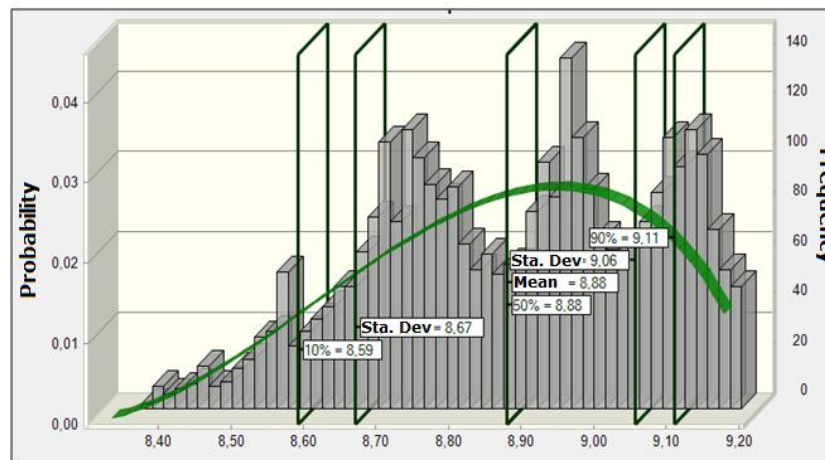
Fig. 4.2. Comparative chart of the effect of electrode distance, positive pulse duration and amplitude of the signal on the uniformity of the electrical potential distribution on the gel-skin interface

Analyzing the reference electrode in the case of the positive pulse duration, the worst uniformity is present when it takes 50% of the period, leaving the other 50% to the negative pulse. This is probably due to the fact that stimulations signals with 30% and 70% Pd stay at a steady value of current density for longer times. Furthermore, applying longer positive pulses and shorter negatives pulses has better results for the uniformity of electrical potential distribution, seeing that Pd=70% provides the best uniformity of the three options in every case, which can be seen most clearly on Signal 1-9, where Pd=70% can have a standard deviation as little as 2.14%. On the other hand, with electrode separation it can be observed how the tendency is to decrease the standard deviation (increase uniformity) with increasing the distance; nevertheless this is variable, as in the case of positive pulse duration, has little effect on the uniformity of the electrical potential distribution along the gel-skin interface. When only the electrode separation is changed in the simulation characteristics, the maximum variation in the standard deviation is from 4.56% (signal 1-7) to 3.83% (signal 1-1). The variable that proves to have more effect on the

uniformity on the electrical potential distribution is the amplitude of the signal; as seen before, this variable can even affect the properties of the tissues, and therefore it is not unexpected that it can alter the electrical potential distribution. It is noted that the lowest standard deviation of 2.14% (signal 1-9) is accomplished with the lowest amplitude studied and reaching a value of 3.48% (signal 4-2) in the signal with highest amplitude studied. Now, analyzing the active electrode gel-skin interface, it can be seen that standard deviation is relatively constant; the electrode distance and positive pulse duration have little effect on the uniformity of the electric potential distribution. The amplitude is again the variable with more affect on the uniformity; signals with amplitude of 3.9417 A/m^2 have the lowest standard deviations but the rest of the studied



(a)



(b)

Fig. 4.3. Probabilistic distribution of the electrical potential RMS values through the gel-skin interface when applying signal 1-9. (a) Active Electrode (b) Reference Electrode

amplitudes show a relatively equal value of standard deviation. The graph clearly shows a higher percentage of dispersion of the data for the active electrode, nevertheless the range (difference between the maximum and minimum values on a data set) for the most dispersed signal (signal 3-2) is only 1.305V, making the differences in electric potential almost negligible. Making a probabilistic study of the surface data sets of the signal with the lowest standard deviation (signal 1-9) with the software Oracle Crystal Ball®, a probabilistic distribution of the data was performed, obtaining the graphs in Fig. 4.3. The reference electrode shows a little dispersed distribution that tend to be in the higher values of electric potential, while the active electrode has a more defined group of preferred values in the low electric potential. To understand the distribution more clearly, a 3D surface graph was obtained for both interfaces as

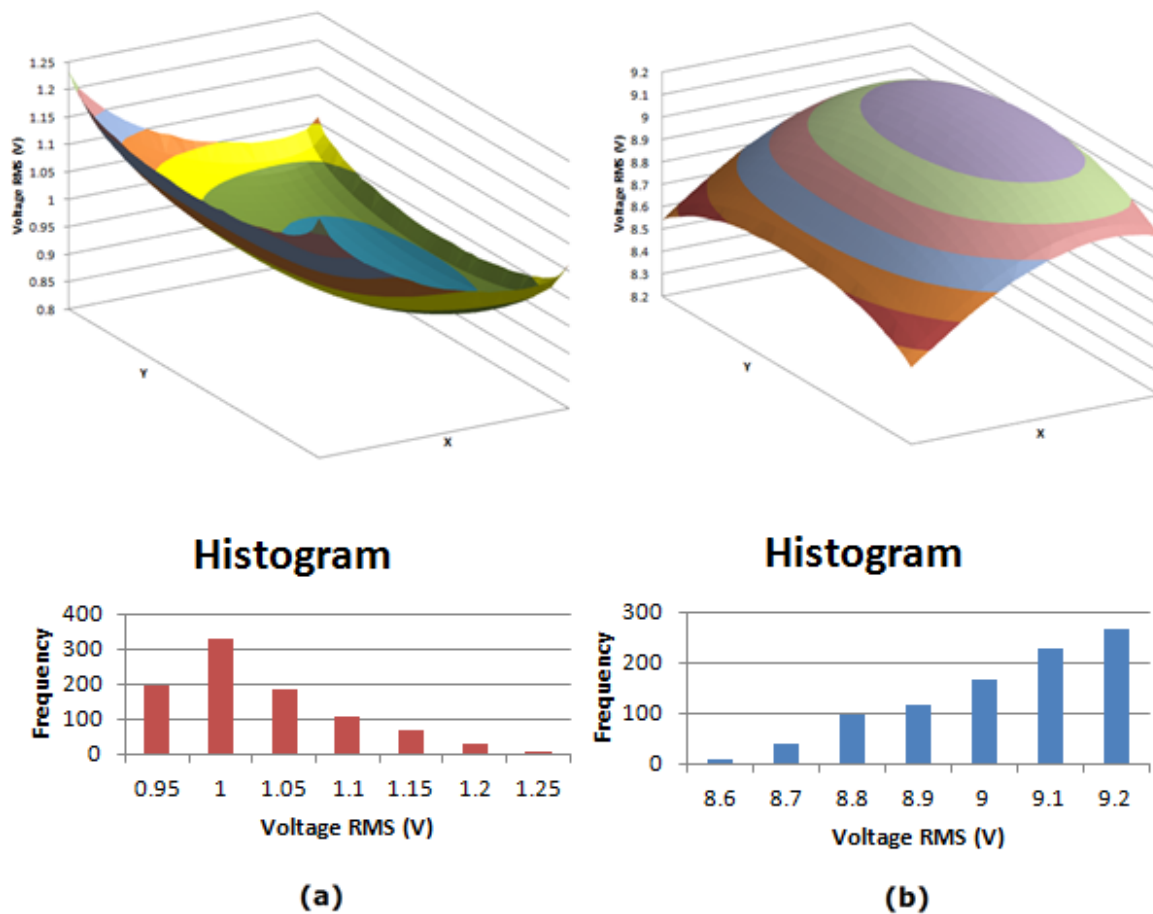


Fig. 4.4. Surface 3D graphs of the electric potential distribution of the gel-skin interface for (a) active electrode and (b) reference electrode observed for signal 1-9

shown on Fig. 4.4, which readily separates areas of the surfaces according to its values and a histogram was created with the frequency of the repetitions for each level of electric potential. For the reference electrode (Fig. 4.4 (b)) it can be seen how the electric potential reaches peak values on an area that is centered and away from the active electrode (most of the nodes on the surface are located on this area) and then the electric potential decreases gradually while approaching the edges of the surface. On the other hand, the active electrode has smaller range of values and most of them on a region between 0.95 and 1.1 V.

4.2 Current Density Distribution

The same study was performed for the current density distribution, using the same Surface “Data Sets” the expression “Current Density Norm” was selected on the “Export” node and the values were exported to Excel to obtain the RMS and statistical values shown on Table 4.3 (Reference electrode) and Table 4.4 (Active electrode). Likewise, a graph summarizing these values was created as shown on Fig 4.5.

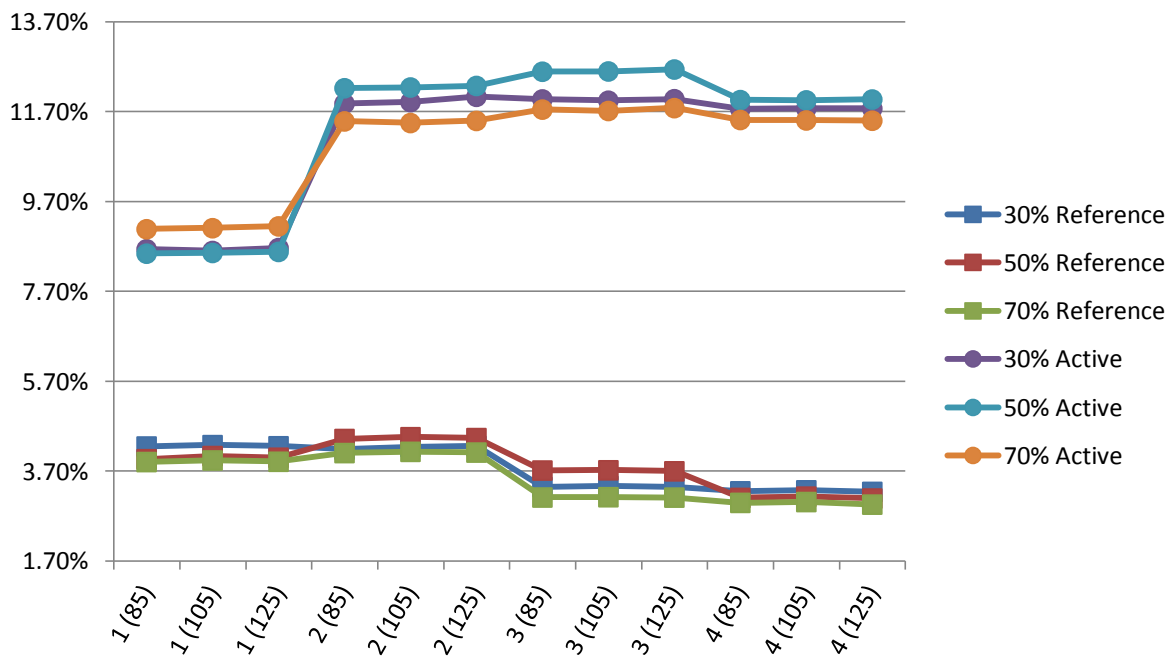


Fig. 4.5. Comparative chart of the effect of electrode distance, positive pulse duration and amplitude of the signal on the uniformity of the current density distribution on the gel-skin interface

Signal ID	Signal Amplitude (A/m ²)	Electrode Separation (mm)	Pd	\bar{X} (A/m ²)	σ (A/m ²)	σ (%)	Range (A/m ²)
1-1	±3.9417	85	30%	3.90993	± 0.16623	4.25%	1.41187
1-2			50%	3.87328	± 0.15373	3.97%	1.40900
1-3			70%	3.90720	± 0.15258	3.91%	1.30379
1-4		105	30%	3.90927	± 0.16741	4.28%	1.44692
1-5			50%	3.86941	± 0.15629	4.04%	1.45427
1-6			70%	3.90708	± 0.15399	3.94%	1.33949
1-7		125	30%	3.90411	± 0.16618	4.26%	1.42420
1-8			50%	3.86874	± 0.15481	4.00%	1.42781
1-9			70%	3.90655	± 0.15282	3.91%	1.32248
2-1	±5.7333	85	30%	3.94339	± 0.16499	4.18%	1.28296
2-2			50%	3.93595	± 0.17392	4.42%	1.35475
2-3			70%	3.92711	± 0.16123	4.11%	1.28380
2-4		105	30%	3.92294	± 0.16638	4.24%	1.29686
2-5			50%	3.93302	± 0.17537	4.46%	1.37073
2-6			70%	3.92642	± 0.16227	4.13%	1.30337
2-7		125	30%	3.92488	± 0.16735	4.26%	1.30788
2-8			50%	3.93531	± 0.17469	4.44%	1.37454
2-9			70%	3.92543	± 0.16159	4.12%	1.30325
3-1	±7.5250	85	30%	7.28119	± 0.24399	3.35%	1.69060
3-2			50%	7.21665	± 0.26821	3.72%	1.86297
3-3			70%	7.19707	± 0.22427	3.12%	1.64064
3-4		105	30%	7.27226	± 0.24519	3.37%	1.69018
3-5			50%	7.26652	± 0.27044	3.72%	1.86629
3-6			70%	7.21598	± 0.22535	3.12%	1.63244
3-7		125	30%	7.27221	± 0.24370	3.35%	1.72900
3-8			50%	7.26508	± 0.26878	3.70%	1.90098
3-9			70%	7.22208	± 0.22491	3.11%	1.66852
4-1	±14.6916	85	30%	13.83194	± 0.45005	3.25%	2.84616
4-2			50%	13.77802	± 0.42804	3.11%	2.68930
4-3			70%	13.53156	± 0.40545	3.00%	2.70001
4-4		105	30%	13.75168	± 0.45050	3.28%	2.85508
4-5			50%	13.73483	± 0.43068	3.14%	2.73331
4-6			70%	13.52910	± 0.40795	3.02%	2.72694
4-7		125	30%	13.82411	± 0.44808	3.24%	2.90195
4-8			50%	13.76324	± 0.42570	3.09%	2.69688
4-9			70%	13.54809	± 0.40075	2.96%	2.75632

Table 4.3. Arithmetic mean (\bar{X}) and standard deviation (σ) of the current density throughout the gel-skin interface located below the reference electrode. Positive pulse duration expressed in percentage of time of the signal period.

Signal ID	Signal Amplitude (A/m ²)	Electrode Separation (mm)	Pd	\bar{X} (A/m ²)	σ (A/m ²)	σ (%)	Range (A/m ²)
1-1	±3.9417	85	30%	4.03786	± 0.34896	8.64%	2.37972
1-2			50%	3.99983	± 0.34176	8.54%	2.39875
1-3			70%	4.05156	± 0.36820	9.09%	2.36373
1-4		105	30%	4.03670	± 0.34733	8.60%	2.37187
1-5			50%	3.99624	± 0.34210	8.56%	2.40225
1-6			70%	4.05267	± 0.36926	9.11%	2.34458
1-7		125	30%	4.03378	± 0.34971	8.67%	2.36508
1-8			50%	3.99697	± 0.34307	8.58%	2.39700
1-9			70%	4.05378	± 0.37098	9.15%	2.34397
2-1	±5.7333	85	30%	4.14560	± 0.49264	11.88%	2.80628
2-2			50%	4.14298	± 0.50656	12.23%	2.95179
2-3			70%	4.12085	± 0.47343	11.49%	2.76642
2-4		105	30%	4.12571	± 0.49174	11.92%	2.79126
2-5			50%	4.14121	± 0.50704	12.24%	2.93190
2-6			70%	4.12007	± 0.47187	11.45%	2.74629
2-7		125	30%	4.13073	± 0.49720	12.04%	2.80459
2-8			50%	4.14501	± 0.50893	12.28%	2.93081
2-9			70%	4.12071	± 0.47386	11.50%	2.73880
3-1	±7.5250	85	30%	7.71184	± 0.92372	11.98%	4.57345
3-2			50%	7.66694	± 0.96563	12.59%	4.91643
3-3			70%	7.61833	± 0.89531	11.75%	4.51106
3-4		105	30%	7.70280	± 0.92047	11.95%	4.50520
3-5			50%	7.72255	± 0.97313	12.60%	4.87643
3-6			70%	7.63868	± 0.89533	11.72%	4.44014
3-7		125	30%	7.70538	± 0.92335	11.98%	4.50503
3-8			50%	7.72416	± 0.97666	12.64%	4.86887
3-9			70%	7.64898	± 0.90138	11.78%	4.44902
4-1	±14.6916	85	30%	14.69395	± 1.72815	11.76%	8.36330
4-2			50%	14.66013	± 1.75382	11.96%	8.39220
4-3			70%	14.36645	± 1.65505	11.52%	8.05956
4-4		105	30%	14.61307	± 1.72049	11.77%	8.18360
4-5			50%	14.61662	± 1.74775	11.96%	8.25125
4-6			70%	14.36629	± 1.65361	11.51%	7.93715
4-7		125	30%	14.69303	± 1.72993	11.77%	8.26058
4-8			50%	14.65172	± 1.75471	11.98%	8.28599
4-9			70%	14.38922	± 1.65540	11.50%	7.95756

Table 4.4. Arithmetic mean (\bar{X}) and standard deviation (σ) of the current density throughout the gel-skin interface located below the active electrode. Positive pulse duration expressed in percentage of time of the signal period.

Data dispersion on the active electrode is very similar to the one observed for the electric potential distribution, showing similar values of standard deviation for variations of Pd and electrode distance but showing better uniformity when applying a signal amplitude of 3.9417 A/m^2 . On the other hand, the data dispersion on the reference electrode differs from the one observed for electric potential distribution. In this case, a relatively constant standard deviation is observed for Pd and electrode distance variation, but there is a slight difference when applying current densities higher than 5.7333 A/m^2 . A probabilistic distribution was also obtained for the current density distribution as shown on Fig. 4.6.

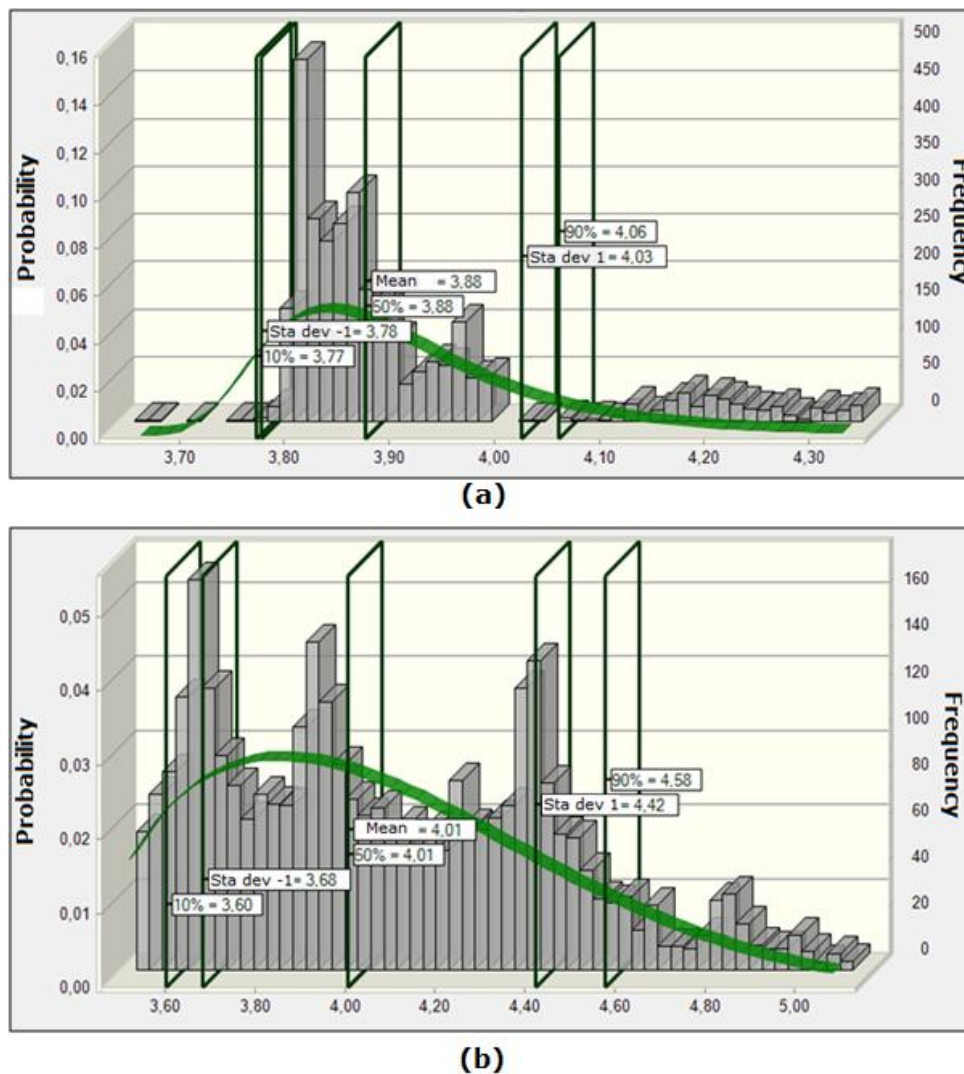


Fig. 4.6. Probabilistic distribution of the current density RMS values through the gel-skin interface when applying signal 1-9. (a) Reference Electrode (b) Active Electrode

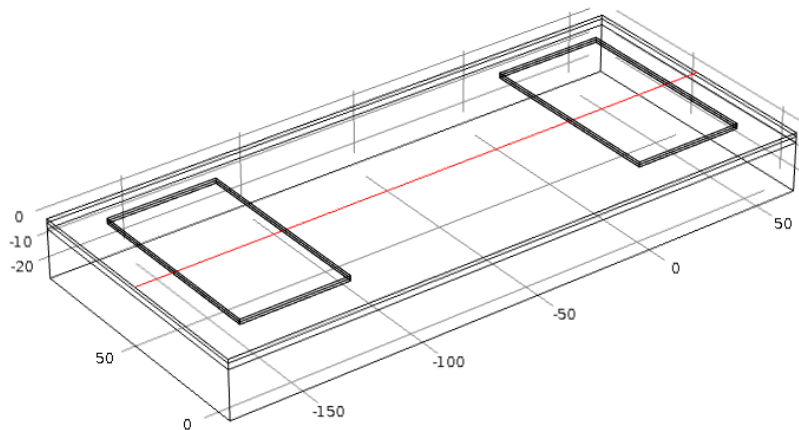


Fig. 4.7. Cut Line Data Set for obtaining current density RMS values

Signal 1-9 was used as example, the same used for the electric potential distribution results. The probabilistic distribution for the gel-skin interface of the active electrode is similar from the one obtained for the electric potential distribution, but with some high peaks obtained for some preferred current density values. Meanwhile, the reference electrode shows high preference for a high value of current density. These high current peaks might be attributed to the edge effect mentioned on Chapter 2 (Kuhn [5]). To observe this effect on the finite element model, a Cut Line Data Set was defined through the center of the geometry as shown on Fig. 4.7 and the values of current density RMS were calculated for the nodes on that line are plotted on Fig. 4.8, and it can be seen how to current density tends to be higher at the edges of the interface below the reference electrode, specially for the inner edge (the one closest to the reference electrode), showing that the edge effect of the electrodes (refer to section 2.4) also affects the current density distribution on the gel-skin interfaces. Using the data set ranges shown on Tables 4.3 and 4.4 it is clear that the higher the amplitude of the stimulation signal the greater is the difference from the lowest value to the highest value of current density, which can be attributed to higher peaks of current on the edges of the gel-skin interface.

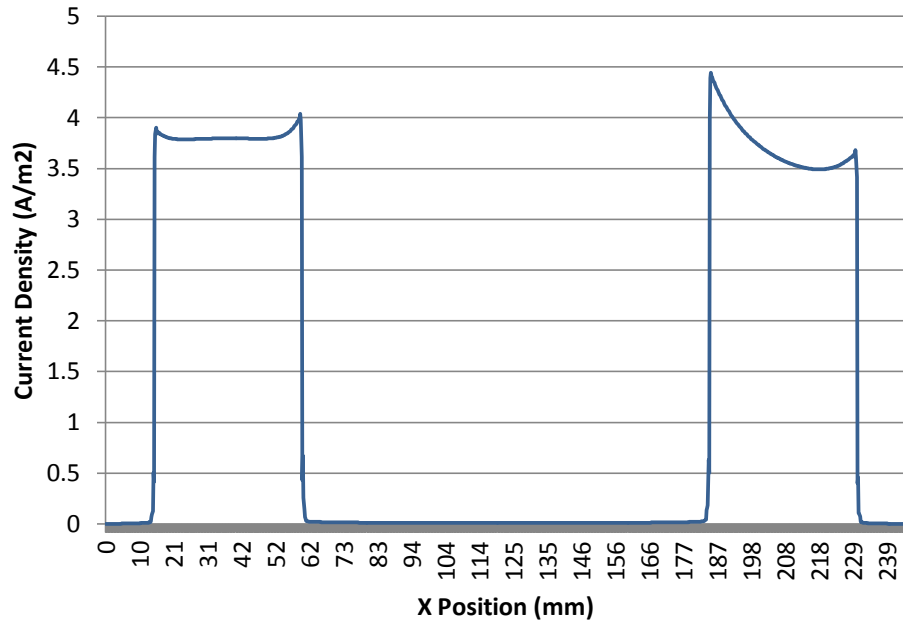


Fig. 4.8. Current Density over the Cut Line Data Set for Signal 1-9

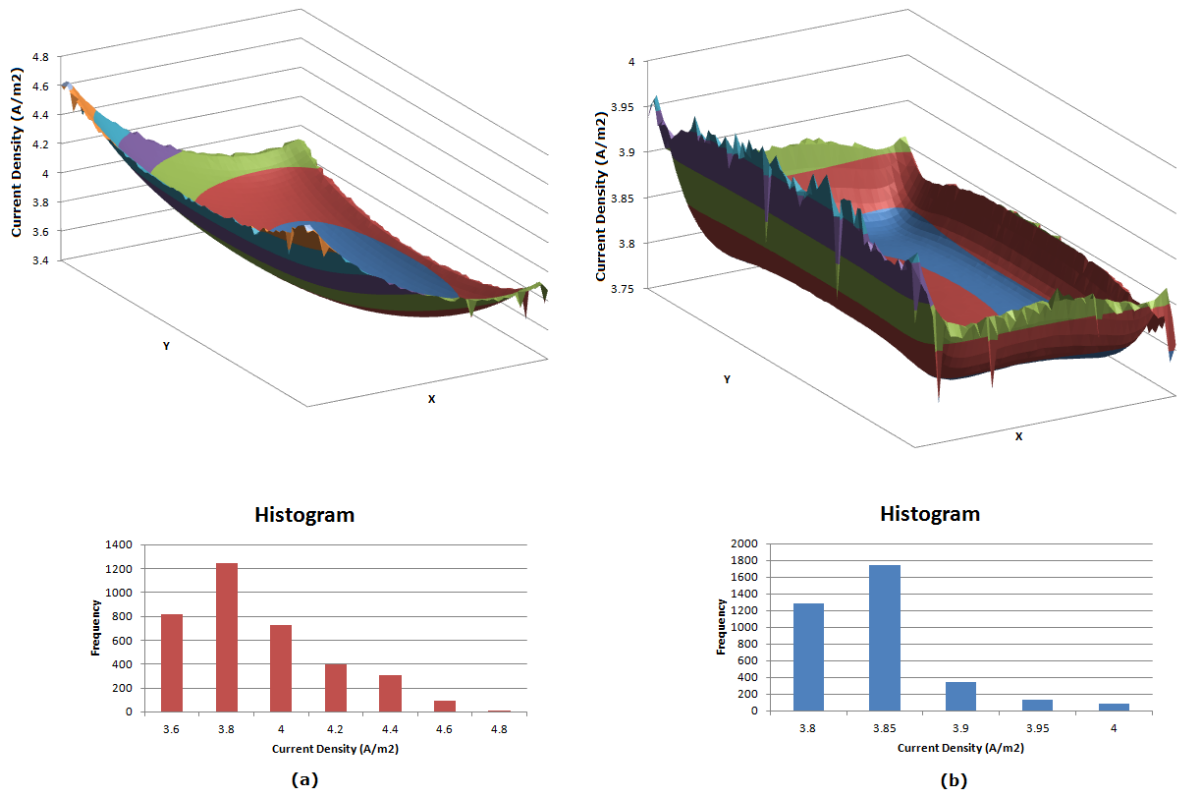


Fig. 4.9. 3D surface graphs of the current density distribution of the gel-skin interface below the (a) active electrode and (b) reference electrode

The same 3D graphs were also created for the current density distribution (Fig.4.9), where the edge effect can also be observed. Given that the exported values necessary for the creation of these graphs that calculated interpolations and due to the rapid variations in current densities, some values at the edges are peaks of low current densities. In these graphs it becomes more evident that the edge effect affects almost exclusively the reference electrode, while the active electrode shows a distribution very much like the one seen for electric potential distribution.

4.3 Total Power Dissipation

In the case of power dissipation, only the 3D surface graphs were obtained to observe the areas with greater power dissipations in the gel-skin interface, this is shown on Fig. 4.10. The power dissipation distribution is very much like the current density distribution, showing peaks of high values for the reference electrode and relatively uniform values for the active electrode. Table 4.5 shows a summary of average power dissipations for all studied cases and Fig. 4.11 is the comparison chart for these values.

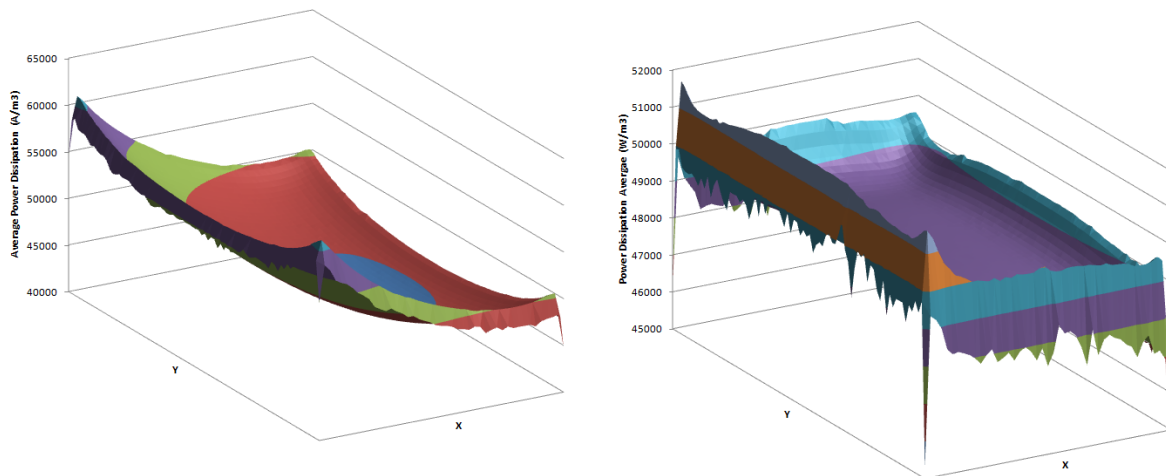


Fig. 4.10. 3D surface graphs for average power dissipation on gel-skin interface below the (a) active electrode and (b) reference electrode

Electrode	Electrode Separation Distance (mm)	Positive Pulse Duration	Average Power Dissipation (W/m)			
			Signal 1	Signal 2	Signal 3	Signal 4
Active Electrode	85	30%	99.2847821	94.8904448	87.1353946	101.014121
		50%	97.9143191	93.3541122	85.254897	94.5553706
		70%	177.902287	169.672601	151.493394	155.984943
	105	30%	99.3418216	94.3981721	87.4057149	97.5997067
		50%	97.9260258	93.6797725	84.7014218	94.2085065
		70%	177.878382	170.331013	150.947394	156.003869
	125	30%	98.8830065	94.5246186	87.1677586	100.969917
		50%	97.3267123	93.0812969	84.9083066	94.2346262
		70%	177.12188	169.574219	150.953221	154.68925
Reference Electrode	85	30%	98.822136	94.5113056	86.2166078	101.014121
		50%	97.4482753	93.2295952	84.3736005	94.5553706
		70%	177.439636	169.915904	150.474649	155.984943
	105	30%	98.8790869	94.5547024	86.4876895	97.5997067
		50%	97.4557631	93.2643325	83.8286122	94.2085065
		70%	177.411452	169.914721	149.934615	156.003869
	125	30%	98.4316249	94.1189294	86.2539106	100.969917
		50%	96.8663425	92.6646927	84.0329953	94.2346262
		70%	176.664843	169.167688	149.943101	154.68925

Table 4.5. Average of the power dissipation throughout the gel-skin interface located below the active and reference electrodes. Positive pulse duration expressed in percentage of time of the signal period

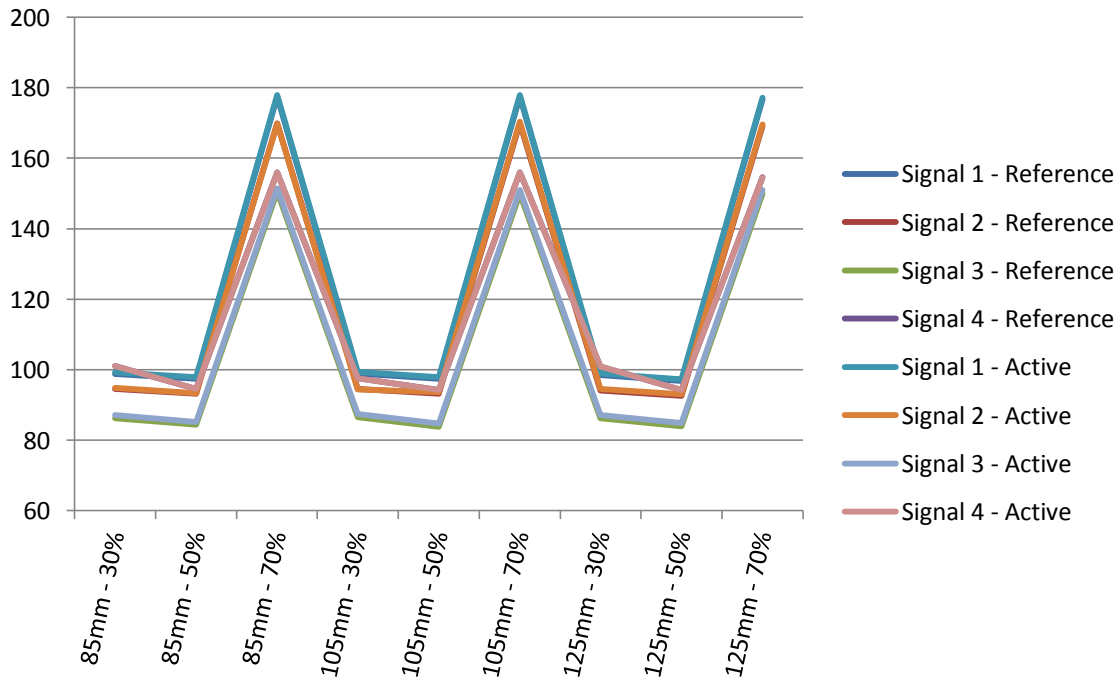


Fig. 4.11. Comparative chart of the effect of electrode distance, positive pulse duration and amplitude of the signal on the average power dissipation on the gel-skin interface

On contrary to electric potential and current density, the amplitude of the signal does not have much effect on the average power dissipation, almost all studied variations have similar values, nevertheless, for $P_d = 70\%$ there are peaks of very high power dissipation that render these signals inefficient in terms of energy, compared to the other options.

Chapter 5

Conclusions and Recommendations

A model for simulating the electrical behavior of the gel-skin interface in NeuroMuscular Electrical Stimulation (NMES) was developed using the COMSOL Multiphysics® software. The Electric Currents Module was used, which employs the Finite Element Method to apply the Maxwell Equations for calculating the electrical potential spatial distribution of a geometry based on resistivity and relative permittivity of its materials.

With the model, 36 different variations of signal properties and electrode configurations were studied (summarized on table 5.1), obtaining the electric potential and current density distributions, as well as average power dissipation of the gel-skin interface.

A uniform distribution of electric potential and current density on the gel-skin interface is important for patient comfort and therapy efficiency. Achieving a higher uniformity would help improve both aspects. The electric potential distribution is more uniform and stable than the current density distribution. The best electric potential distribution is achieved with longer electrode separation distances, smaller stimulation signal amplitude and positive pulse duration of 70% or 30% of the time of the period (positive pulse duration of 50% showed the worst results). For the evaluated cases, the signal with best electric potential distribution uniformity is signal 1-9 with stimulation signal amplitude of 3.9417 A/m^2 , positive pulse duration of 70% and an electrode separation distance of 125mm. The current density distribution on the active electrode is also relatively uniform; resembling the one seen for the electric potential, but the

reference electrode is greatly affected by electrode edge effects, presenting high peaks of current on the edges of the interface. For both electrodes, a lower stimulation signal amplitude provides a good uniformity, nevertheless the electrode separation distance and positive pulse duration make practically no difference, making all signals with the lowest amplitude (3.9417A/m²) a good choice. The current density distribution exerts the greatest effect on power dissipation, given that both spatial distributions are very alike (higher at the edges). Further, the average power dissipation is very similar for all variations of amplitude and electrode separation distances but it spikes at positive pulse durations of 70%. Taking into account all three variables (electric potential, current and power) it would be signal 1-7 the one with the best global uniformity and energy efficiency with amplitude of 3.9417 A/m², electrode separation of 125mm and positive pulse duration of 30%.

Unfortunately, these signal properties and electrode configuration can't be applied to every muscle and patient; amplitude of 3.9417 A/m² might achieve too little muscle fiber recruitment and the muscle might not be large enough to place the electrodes 125mm apart and such a separation might not provide very good accuracy (not region specific). Therefore, the guidelines to achieve good distribution uniformity would be:

- 1) Apply low amplitude stimulation signals
- 2) Place electrode as far apart as possible without compromising stimulation accuracy
- 3) Apply stimulation signals with positive pulse durations (or duty cycles for monophasic signals) lower than 50%

The described model was developed to be easily customizable, so it might also be used to further study other types of stimulation waves (triangular, sine, monophasic), electrode configurations and sizes and material properties by simply changing the parameters described on Chapter 3. This could provide a way to save on experimentation time and expenses by narrowing down the independent variables of experimentation to the most promising ones.

Finally, it is recommended to explore other output expressions in the results node of COMSOL to obtain more useful information about the simulations performed with the described model.

REFERENCES

- [1] L. Sherwood, *Human Physiology: From Cells to Systems*, 7th ed. CENGAGE Learning, 2004.
- [2] D. L. Villarreal, D. Schroeder, and W. H. Krautschneider, “Equivalent Circuit Model to Simulate the Neuromuscular Electrical Stimulation Nerve and Muscle Stimulation with Simulation Comparison,” in *ICT Open Proceedings. Electronic Circuits and Systems (ProRISC)*, 2012, pp. 46–52.
- [3] E. Henneman, G. Somjen, and D. Carpenter, “Functional significance of cell size in spinal motoneurons,” *J. Neurophysiol.*, vol. 28, no. 3, pp. 560–580, 1965.
- [4] C. M. Gregory and C. S. Bickel, “Recruitment patterns in human skeletal muscle during electrical stimulation.,” *Phys. Ther.*, vol. 85, no. 4, pp. 358–64, Apr. 2005.
- [5] A. Kuhn, “Modeling Transcutaneous Electrical Stimulation,” ETH Zurich, 2008.
- [6] G. E. Loeb and R. a Peck, “Cuff electrodes for chronic stimulation and recording of peripheral nerve activity.,” *J. Neurosci. Methods*, vol. 64, no. 1, pp. 95–103, Jan. 1996.
- [7] J. A. Hoffer and G. E. Loeb, “Implantable electrical and mechanical interfaces with nerve and muscle,” *Ann. Biomed. Eng.*, vol. 8, pp. 351–360, 1980.
- [8] M. S. George, H. a Sackeim, a J. Rush, L. B. Marangell, Z. Nahas, M. M. Husain, S. Lisanby, T. Burt, J. Goldman, and J. C. Ballenger, “Vagus nerve stimulation: a new tool for brain research and therapy.,” *Biol. Psychiatry*, vol. 47, no. 4, pp. 287–95, Feb. 2000.
- [9] B.-P. Bejjani, P. Damier, I. Arnulf, L. Thivard, A.-M. Bonnet, D. Dormont, P. Cornu, B. Pidoux, Y. Samson, and Y. Agid, “Transient Acute Depression Induced by High-Frequency Deep-Brain Stimulation,” *N. Engl. J. Med.*, vol. 340, no. 19, pp. 1476–1480, May 1999.
- [10] B. Cross and B. Shield, “Percutaneous Electrical Nerve Stimulation (PENS) or Neuromodulation Therapy,” vol. 510. pp. 1–5, 2012.
- [11] W. F. Craig, P. F. White, H. E. Ahmed, B. N. Henderson, P. J. Huber, and R. J. Gatchel, “Percutaneous Electrical Nerve Stimulation for Low Back Pain,” *J. Am. Med. Assoc.*, vol. 281, no. 9, pp. 818–823, 1999.
- [12] D. G. Greathouse, “Electrotherapeutic Terminology in Physical Therapy,” *J. Orthop. Sport. Phys. Ther.*, vol. 23, no. 4, p. 233, Apr. 1996.
- [13] K. A. Sluka and D. Walsh, “Transcutaneous Electrical Nerve Stimulation: Basic Science Mechanisms and Clinical Effectiveness,” *J. Pain*, vol. 4, no. 3, pp. 109–121, 2003.
- [14] D. Beckwée, W. De Hertogh, P. Lievens, I. Bautmans, and P. Vaes, “Effect of tens on pain in relation to central sensitization in patients with osteoarthritis of the knee: study protocol of a randomized controlled trial.,” *Trials*, vol. 13, no. 1, p. 21, Jan. 2012.

- [15] N. a Maffiuletti, M. a Minetto, D. Farina, and R. Bottinelli, "Electrical stimulation for neuromuscular testing and training: state-of-the art and unresolved issues.," *Eur. J. Appl. Physiol.*, vol. 111, no. 10, pp. 2391–7, Oct. 2011.
- [16] E. A. Blair and J. Erlanger, "A comparison of the characteristics of axons through their individual electrical responses," *Am. J. Physiol. Content*, vol. 106, no. 3, pp. 524–564, 1933.
- [17] J. P. Porcari, K. P. McLean, C. Foster, T. Kernozek, B. Crenshaw, and C. Swenson, "Effects of electrical muscle stimulation on body composition, muscle strength, and physical appearance.," *J. Strength Cond. Res.*, vol. 16, no. 2, pp. 165–72, May 2002.
- [18] C. Bickel, J. Slade, G. Warren, and G. Dudley, "Fatigability and variable-frequency train stimulation of human skeletal muscles," *Phys. Ther.*, vol. 83, no. 4, pp. 366–373, 2003.
- [19] M. H. Trimble and R. M. Enoka, "Mechanisms underlying the training effects associated with neuromuscular electrical stimulation.," *Phys. Ther.*, vol. 71, no. 4, pp. 273–80; discussion 280–2, Apr. 1991.
- [20] W. F. Brown, C. F. Bolton, and M. J. Aminoff, *Neuromuscular function and disease: basic, clinical, and electrodiagnostic aspects*, vol. 1. Elsevier Health Sciences, 2002.
- [21] D. Villarreal Lujan, "Equivalent Circuit Model to Simulate the Neuromuscular Electrical Stimulation," Technische Universitat Hamburg-Harburg, 2010.
- [22] A. Hadzic and J. Vloka, *Peripheral nerve blocks: principles and practice*. McGraw-Hill/Professional, 2004.
- [23] T. Keller and A. Kuhn, "Electrodes for transcutaneous (surface) electrical stimulation," *J. Autom. Control*, vol. 18, no. 2, pp. 35–45, 2008.
- [24] E. Mcadams, *Bio-Medical CMOS ICs*. Boston, MA: Springer US, 2011, pp. 31–124.
- [25] J. Bensouilah and P. Buck, "Skin Structure and Function," in in *Aromadermatology: Aromatherapy in the Treatment and Care of Common Skin Conditions*, Journal of the Australian Traditional-Medicine Society, 2007.
- [26] J. McGrath, R. Eady, and F. Pope, "Anatomy and organization of human skin," *Rook's Textb. ...*, 2010.
- [27] T. Yamamoto and Y. Yamamoto, "Electrical properties of the epidermal stratum corneum.," *Med. Biol. Eng.*, vol. 14, no. 2, pp. 151–8, Mar. 1976.
- [28] J. F. Lane, "Electrical impedances of superficial limb tissues: epidermis, dermis and muscle sheat," *Ann. N. Y. Acad. Sci.*, vol. 170, no. 2, pp. 812–825, 1970.
- [29] T. SUCHI, "Experiments on electrical resistance of the human epidermis.," *Jpn. J. Physiol.*, vol. 5, no. 1, p. 75, 1955.
- [30] L. A. Geddes and L. E. Baker, *Principles of applied biomedical instrumentation*. Wiley Online Library, 1975.
- [31] V. G. Gusev, a I. Demin, L. M. Galina, and E. S. Mikhal'chenko, "A study of electrical properties of human skin," *Med. Tekh.*, vol. 43, no. 3, pp. 20–4, 2009.

- [32] M. Damijan, P. Natasa, and F. X. Hart, “Electric properties of tissues,” *Wiley Encyclopedia of Biomedical Engineering*. pp. 1–12, 2006.
- [33] C. Furse, D. Christensen, and C. Durney, *Basic Introduction to Bioelectromagnetics*, 2nd Editio. CRC Press, 2009.
- [34] E. Barkanov, “Introduction to the Finite Element Method.” Institute of Materials and Structures of Riga Technical University, 2001.
- [35] D. Roylance, “Finite element analysis.” Massachusetts Institute of Techonology, 2001.
- [36] R. D. Cook, D. S. Malkus, M. E. Plesha, and R. J. Witt, *Concepts & Applications of Finite Element Analysis*, 4th ed. John Wiley & Sons, INC, 2002.
- [37] COMSOL, “AC/DC Module User’s Guide,” in in *COMSOL User’s Guide*, 2012.
- [38] L. L. Baker, B. R. Bowman, and D. R. McNeal, “Effects of waveform on comfort during neuromuscular electrical stimulation.,” *Clin. Orthop. Relat. Res.*, no. 233, pp. 75–85, 1988.
- [39] C. Boccaletti, G. Fabbri, M. Santello, and O. Street, “A NON-INVASIVE BIOPOTENTIAL ELECTRODE FOR THE,” in *Sixth IASTED International Conference*, pp. 353–558.